OFFICE OF NAVAL RESEARCH

Contract N00014-84-K-0021

Technical Report No. 20

Anomalous Stresses vs. Extent of Cure in an Epoxy composite Specimen

by

M. A. Taylor and J. K. Gillham

Polymer Materials Program
Department of Chemical Engineering
Princeton University
Princeton, NJ 08544

June 1989

Principal Investigator
John K. Gillham
(609) 452-4694

SECURITY CLASSIFICATION OF THIS PAGE (When Data Entered)

REPORT DOCUMENTATION PAGE

READ INSTRUCTIONS BEFORE COMPLETING FORM

1 REPORT NUMBER: Technical Report # 20	2 GOVT ACCESSION NO.: N/A	3 RECIPIENT'S CATALOG NUMBER: N/A
4 TITLE (and Subtitle): Anomalous Stresses vs. Extent of Cure in an Epoxy Composite Specimen		5 TYPE OF REPORT & PERIOD COVERED: 1/7/88 - 6/15/89
		6 PERFORMING ORG. REPORT NUMBER:
7 AUTHOR(s): M. A. Taylor and M. K. Gillham		8 CONTRACT OR GRANT NUMBER(s): N00014-84-K-0021
9 PERFORMING ORGANIZATION NAME AND ADDRESS: Polymer Materials Program, Department of Chemical Engineering, Princeton University, Princeton, NJ 08544		10 PROGRAM ELEMENT, PROJECT, TASK AREA & WORK UNIT NUMBERS:
11 CONTROLLING OFFICE NAME AND ADDRESS: Office of Naval Research, Attn: Code 413, 800 N. Quincy St., Arlington, VA 22217		12 REPORT DATE: June 1989 13 NUMBER OF PAGES: 41
14 MONITORING AGENCY NAME & ADDRESS (if different from Controlling Office)		15 SECURITY CLASS. (of this report): Unclassified 15a DECLASSIFICATION/DOWNGRADING SCHEDULE:

16 DISTRIBUTION STATEMENT (of this Report)

Approved for public release; distribution unlimited.

17 DISTRIBUTION STATEMENT (of the abstract entered in Block 20, if different from Report)

N/A

18 SUPPLEMENTARY NOTES

19 KEY WORDS (Continue on reverse side if necessary and identify by block number)

Stresses	Density
Cure	Torsional Braid Analysis
Vitrification	Epoxy
Glass Transition	Dynamic Mechanical Analysis

20 ABSTRACT (Continue on reverse side if necessary and identify by block number)

Recent studies on the properties of high T_g epoxy systems (i.e., difunctional aromatic epoxy resins cured with tetrafunctional aromatic diamines) have shown that, with increasing conversion, the room temperature density increases prior to gelation but decreases after gelation. The lower room temperature modulus and higher equilibrium moisture absorption at higher conversions have been attributed to the lower density. The anomalous behavior has been explained using the concept of free volume and the non-linear increase of Tg with conversion. The present study relates the anomalous changes in density and

DD FORM 1 JAN 73 1473 EDITION OF 1 NOV 65 IS OBSOLETE
S/N 0102-014-6601

SECURITY CLASSIFICATION OF THIS PAGE (When Data Entered)

(block number 20 continued)

modulus to the bending developed in a bilayer epoxy system/silicon wafer composite specimen using a cantilever beam technique. The results demonstrate that the room temperature stress also passes through a maximum with increasing conversion.

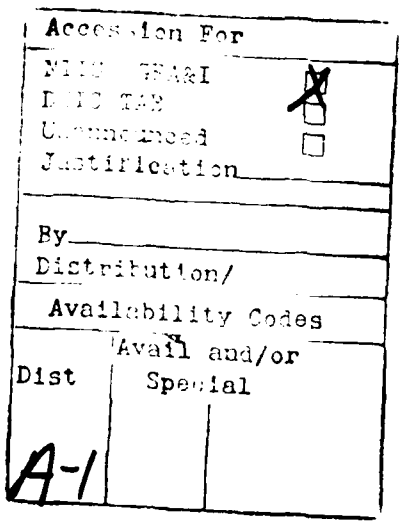

ANOMALOUS STRESSES VS. EXTENT OF CURE IN AN EPOXY COMPOSITE SPECIMEN

M. A. Taylor and J. K. Gillham, Polymer Materials Program, Department of Chemical Engineering, Princeton University, Princeton, NJ 08544.

SYNOPSIS

Recent studies on the properties of high T_g epoxy systems (i.e., difunctional aromatic epoxy resins cured with tetrafunctional aromatic diamines) have shown that, with increasing conversion, the room temperature density increases prior to gelation but decreases after gelation. The lower room temperature modulus and higher equilibrium moisture absorption at higher conversions have been attributed to the lower density. The anomalous behavior has been explained using the concept of free volume and the non-linear increase of T_g with conversion. The present study relates the anomalous changes in density and modulus to the bending developed in a bilayer epoxy system/silicon wafer composite specimen using a cantilever beam technique. The results demonstrate that the room temperature stress also passes through a maximum with increasing conversion.

INTRODUCTION

An isothermal time-temperature-transformation (TTT) cure diagram (Fig. 1) can be used as a tool to study relationships between curing phenomena of thermosetting resins and physical properties (1). The cure diagram is constructed from the times to events that occur during isothermal cure at different temperatures (T_c). The time-temperature plot is separated into four distinct states of the thermosetting-cure

process by the gelation contour and the vitrification contour. These states are liquid, gelled rubber, ungelled glass and gelled glass. $T_{g\infty}$ is the glass transition temperature (T_g) of the fully cured resin (above which the fully cured material is a rubber), ${}_{gel}T_g$ is the temperature at which vitrification and molecular gelation occur simultaneously (i.e., the glass transition temperature of the molecular gel point). Similarly, ${}_{gel}T_g'$ is the temperature at which vitrification and macroscopic gelation occur simultaneously, and T_{go} is the glass transition temperature of the unreacted resin mixture. The torsional braid analysis (TBA) technique has been employed in the direct determination of the times of vitrification and gelation from the maxima of the loss peaks in isothermal dynamic mechanical spectra (2). As the cure reaction proceeds, viscosity, relative rigidity (~ modulus), and density increase at the temperature of reaction as a result of increasing molecular weight and crosslinking. The reaction becomes diffusion-controlled as the material vitrifies (i.e., when $T_g = T_c < T_{g\infty}$). The cure temperature (T_c) and cure time (t_{cure}) strongly influence properties such as room temperature density, modulus and equilibrium water absorption (3,4,5).

Investigations of the properties of difunctional aromatic epoxy resins cured with tetrafunctional aromatic diamines have shown that with increasing conversion, the room temperature density (ρ_{RT}) increases prior to gelation but decreases after gelation (e.g.,6). The lower room temperature modulus and higher equilibrium moisture absorbed at long cure times are also a consequence of lower ρ_{RT} (3,4). The anomalous behavior has been explained using the concept of free volume, and the non-linear increase of T_g with conversion (Fig. 2) (6). Theoretical treatments of the anomalous behavior have been reported (4-8). For example (6), the

following parameters have been defined from the slopes of specific volume versus temperature curves:

$$E_L = [V(T_c) - V(T_g)]/(T_c - T_g) \quad (1)$$

$$E_G = [V(T_g) - V(RT)]/(T_g - RT) \quad (2)$$

where $V(T_c)$ = specific volume at temperature of cure

T_c = temperature of cure

$V(T_g)$ = specific volume at T_g

$V(RT)$ = specific volume at RT

From equations (1) and (2), the specific volume at room temperature is given as

$$V(RT) = V(T_c) - E_L(T_c - T_g) - E_G(T_g - RT) \quad (3)$$

which assumes that the expansion coefficients in the rubbery (L) and glassy (G) states do not change with extent of cure (5-7). Figure 3 shows schematically the effect of extent of cure on volume-temperature behavior (6). With increasing cure at low conversions, T_{g1} increases to T_{g2} and $V(RT_1)$ decreases to $V(RT_2)$, as expected. However, above temperature $_{gel}T_g$, as T_{g2} increases rapidly to T_{g3} at a higher extent of cure, $V(RT_2)$ *increases* to $V(RT_3)$. This latter behavior represents the anomaly. Differentiating equation (3) with respect to the extent of cure (x), yields

$$dV(RT)/dx = dV(T_c)/dx + (E_L - E_g)dT_g/dx \quad (4)$$

From equation (4), the relative magnitudes of $dV(T_c)/dx$ (which is negative) and $(E_L - E_g)dT_g/dx$ (which is positive) will determine whether the specific volume at room temperature decreases, remains unchanged, or increases (6). It is apparent that the effect of increasing glass transition temperature at higher conversions can dominate the effect of shrinkage due to cure. This occurs when the shrinkage due to chemical cure at T_c is smaller than the contraction on cooling; the specific volume at room temperature then increases according to Eq. (4). Under these conditions, the expected decrease in free volume associated with higher extents of cure is negated. Consequently, ρ_{RT} decreases.

Since dimensional changes and modulus influence the bending of an epoxy composite specimen, an attempt is made in this study to determine whether the anomalous behavior in RT density can be related to the RT stresses associated with the bending of a cantilevered bilayer specimen (epoxy coating/silicon wafer).

Theory of the Horizontal Cantilever Method

Our assumption in using a bilayer composite of coating on a substrate in the cantilever beam experiment is that dimensional changes of one component relative to the other (due to cure and thermal coefficients) will result in stresses which produce bending, the extent of which is determined by differences in the densities and moduli of the components. The changing density and modulus of the coating relative to the substrate lead to tensile and compressive stresses in the film and substrate, respectively.

The curvature of the composite specimen is determined by measuring the divergence of two laser beams which are originally parallel. Changes in spot separation of the beams on a detector are related to curvature, K, by

$$K = \frac{\delta}{2dS} \tag{5}$$

where K = 1/R, R = radius of curvature, δ is the change in the spot separation of the reflected beam, d is the original separation of the parallel laser beam, and S is the distance from the sample to the detector (9). From Stoney (10), and Wilcock (11), the curvature is related to stresses by

$$\sigma = \frac{E(t_s)^2}{6Rt_d(1-\upsilon)} \tag{6}$$

where σ is the stress in the polymer film, t_d is the film thickness, t_s is the thickness of the substrate, and E and υ are the Young's modulus and the Poisson ratio, respectively, of the substrate. Eq. (6) is based on the following assumptions (11): 1) the curvature of the substrate is much less than its thickness; 2) the substrate thickness is greater than or equal to the film thickness; 3) the width of the substrate is less than half the length, and 4) the Young's moduli of the film and the substrate are the same order of magnitude.

All the assumptions were reasonably satisfied in this study, as is evident from the following: the thickness of the substrate (t_s) = 0.02 cm,

the lowest substrate curvature = 0.14 cm^{-1}, the maximum film thickness (t_d) = 0.02 cm (minimum = 0.013 cm), and the lateral dimensions of the substrate = 0.5 cm x 3.0 cm. Young's modulus of the silicon wafer = 3.5 x 10^{10} dyne/cm^2 (9), whereas typical values of the modulus for fully cured epoxies range from 2.8 x 10^{10} to 4.1 x 10^{10} dyne/cm^2 (12).

EXPERIMENTAL

Materials

The epoxy system used in this research was a difunctional epoxy resin (diglycidyl ether of bisphenol A, DER 332, Dow Chemical Company) cured with a tetrafunctional aromatic diamine (trimethylene glycol di-p-aminobenzoate, TMAB, Polarcure, 740M, Polaroid Corp.) (Fig. 4). The equivalent weights of the epoxy monomer and the curing agent are 173 gm/eq. and 78.5 gm/eq., respectively. The epoxy monomer is a viscous liquid at room temperature. The curing agent has a melting point of 125°C. Stoichiometric amounts of the epoxy monomer and the curing agent were mixed in a beaker mechanically at 100°C for 15 minutes. The formulation was transferred into aluminum pans which were placed in a desiccator, and stored in a freezer.

Experiments were carried out by spin-coating the epoxy formulation on silicon wafer substrates. The epoxy mixture was coated on the unpolished side of the wafer; the spin coater was allowed to spin for about 2 minutes. An infra-red lamp was focused on the sample to ensure effective coating by reducing the viscosity of the formulation.

For the density measurements, disc-shaped cast specimens (average diameter ca. 5 mm; average thickness ca. 1 mm; average weight ca. 25 mg) were cured in an aluminum foil-lined mold. In effect, the procedure

follows that reported (6), except that the aluminum foil with its specimens was free-cooled to room temperature in a dessicator for 1 hour prior to density measurements.

Stress Measurements

The cantilever beam technique included parallel laser beams which were obtained from a single-mode He-Ne laser and beam-splitter prism configuration arranged on an optical bench (Fig. 5). The two beams were chopped mechanically so that they fell alternately on the composite specimen. A furnace tube of sufficient diameter to allow the entry and exit of both laser beams was clamped at one end of the optical bench. The specimen holder, a ceramic tube, was clamped at the other end of the bench in such a way that it could be moved in and out of the furnace tube. A thermocouple was used near the clamped end of the furnace tube to monitor the temperature of cure. The clamped end of the furnace tube diverges into two separate smaller tubes to allow the intermittent flow of heated or cooled nitrogen gas.

Below the furnace tube is a clamped mirror at an angle of 45°. The beams, after impinging on the mirror and the shiny surface of the composite specimen, are reflected across the room to a position detector. A standard lock-in amplifier measured the voltage which corresponded to the spot separation. Changes in spot separation corresponded to changes in curvature and to changes in the stresses developed in the composite specimen. An IBM-PC computer was used for data acquisition and processing (9,13,14).

For measurements of the stress at room temperature after cure, the specimen was cured isothermally at a given temperature and then cooled

freely to room temperature (ca. 5°C/min). Measurements were made one hour after the start of cooling.

Density Measurements

Densities of the cured specimens were determined in a density gradient column (6) prepared from toluene and carbon tetrachloride. The column was calibrated with density floats of known density (Fig. 6). The temperature of the density column was maintained at 24.95 ± 0.05°C using circulating water. The sensitivity of the column was maintained at 0.0005 g/mL cm.

Prior to immersion in the density gradient column, specimens were examined between a pair of polarizers under a microscope to ensure the absence of visible voids and bubbles. Three to four specimens with the same prehistory were carefully dropped into the density column. Readings were taken after 30 minutes. At this time, their heights in the column had remained constant for about 10 minutes (also, see Fig. 24).

Torsional Braid Analysis (TBA)

Data for the TTT cure diagram were obtained by using the torsional braid analyzer (TBA) technique (2). A time-temperature-transformation (TTT) cure diagram for DER 332/TMAB (Fig. 7) was constructed (15) by assigning the times to vitrification and macroscopic gelation from the maxima in logarithmic decrement versus isothermal cure time plots. $T_{g\infty}$ and ${}_{gel}T_g'$ of this epoxy system are approximately 180°C and 35°C, respectively. The TTT cure diagram was used as a framework to relate the effects of cure time and cure temperature on room temperature density and stress.

It is interesting to note that the TBA technique itself has been used to monitor the effects of dimensional changes of one component on the stresses developed in a composite specimen, in a similar manner to the present use of the bilayer composite specimen. A typical TBA specimen consists of a heat-cleaned glass braid impregnated with a polymeric matrix; the composite specimen supports an inertial mass, the angular position of which is measured. For example, it has been reported that a cellulose triacetate/glass braid TBA specimen will spontaneously rotate torsionally in one direction as the polymer expands (e.g. through T_g and T_m); it will spontaneously rotate torsionally in the other direction as the polymer contracts (e.g., through crystallization and crosslinking) (16).

RESULTS

Stress vs. Time and Temperature of Isothermal Cure

The raw data for a composite specimen during cure at an isothermal temperature of 120°C are plotted as change in spot separation of the parallel laser beams vs. time of cure (Fig. 8). The same data (Fig. 8) are used to calculate the change in curvature of the composite specimen (Eq. 6) during isothermal cure (Fig. 9). This shows continual bending for times greater than 4 hours until the curvature is independent of cure time after about 20 hours. The change in stress associated with the bending of the composite specimen is calculated (Eq. 7) and plotted against time of isothermal cure (Fig. 10). The increase in stress is due to physical densification (i.e., shrinkage) of the epoxy film as it is transformed from the liquid or rubbery state to glass (6). Figures 11, 12 and 13 show change in spot separation, change in curvature, and change in stress during a temperature scan (50 to 250°C, as described in the corresponding Figure

captions), respectively, of a specimen with initially uncured epoxy. The developed isothermal time-dependent stresses (Fig. 10) are of higher magnitude than the temperature-dependent stresses (Fig. 13), since the former involve only isothermal (cure) shrinkage whereas the latter involve the net effect of expansion on heating and cure shrinkage.

Figure 14 shows the change in room temperature (RT) stress versus time of cure at an isothermal temperature of 120°C. The developed room temperature stress increases to a maximum value and then decreases with increasing cure time. The changes in stress at RT are the net result of the consequence of cure shrinkage at the temperature of cure and of the mismatch of the thermal coefficients of the epoxy film and substrate on cooling to RT. Figures 15 and 16 and 17 show the developed room temperature stress versus time of cure at 130, 140 and 160°C, respectively. The observations are similar to those of Figure 14. A summary of the changes in room temperature stress vs. time of cure at different isothermal cure temperatures (120 to 160°C) is shown in Figure 18. The increase in room temperature stress for partially cured specimens appears to be insensitive to the particular temperatures of cure. However, the limiting level of the change in room temperature stress (at long times) decreases with increasing cure temperature, presumably because of the higher conversions required to vitrify the material at higher temperatures.

Comparison of the summarizing data of Figure 18 and the TTT cure diagram of Figure 7 shows that the maxima in the developed room temperature stress occur after vitrification. The relative insensitivity of the times of the maxima to the particular cure temperatures is

presumably the consequence of the similar times to vitrify at the different temperatures.

Density at Room Temperature vs. Time and Temperature of Isothermal Cure

Data for specimens which had been cured at various temperatures for different times and cooled to RT are presented in this section. A plot of room temperature density, ρ_{RT}, versus cure time at an isothermal temperature of 120°C is shown in Fig. 19. The room-temperature density increases with cure time to a maximum value and then decreases with further cure until it reaches a limiting value. Comparison of the data of Fig. 19 and Fig. 7 shows that, for cure at 120°C, the maximum in ρ_{RT} occurs after isothermal vitrification and corresponds with the maximum in the developed room temperature stress, both occurring after ca. 630 minutes of cure. The TBA results (Fig. 7) show at 120°C that macroscopic gelation occurs at ca. 40 min. and vitrification occurs at ca. 500 min.

Studies performed in this laboratory on another epoxy system showed that ρ_{RT} passed through a maximum in the vicinity of gelation (6), a conclusion which differs from the present report. The present material undergoes gelation well before the maximum room-temperature density is achieved. This conclusion is supported by a simple experiment in which the location in the density gradient column of specimens cured for different cure times at 120°C was monitored vs. time of immersion in the density gradient column (Fig. 24). Specimens, which had been cured for 30 minutes at 120°C, dropped slowly to the bottom of the column (and eventually dissolved); this is due to gelation of the material not occurring at cure times of 30 minutes (see TTT diagram). Long term

results using the density gradient column show that molecular gelation occurs between 0.5 and 1 hour at T_c = 120°C (see Fig. 24).

The data (Fig. 24) for the density gradient column at early times of immersion (i.e., before the glassy specimens had absorbed solvent) also confirm the density changes seen in Figure 19. Specimens cured for 12 hour at 120°C (which coincides with the time of cure for maximum RT density) also show the highest density (lowest location in the column). More fully cured specimens (168 hr.) confirmed the decreasing room-temperature density with increasing extent of cure. The anomaly was not observed for specimens left in the density gradient column for 1400 min (ca. 1 day) since the densities are then the equilibrium measurements of solvent-swollen polymer in the rubbery state.

Figures 20, 21 and 22 show similar trends of decreasing room-temperature density (measured in the density gradient column after 30 minutes of immersion) with increasing cure times at 130, 140 and 160°C, respectively. A summary of the room-temperature density vs. cure time at different isothermal temperatures is presented in Figure 23.

The maxima in ρ_{RT} correspond to the maxima in the developed room temperature stress. The ρ_{RT} vs. t_{cure} data for various T_cs (like the corresponding RT stress vs. t_{cure} data for various T_cs) are not very sensitive to the chosen values of T_c (presumably because the vitrification times for the selected T_cs are similar). Long periods of isothermal cure to well beyond vitrification result in limiting values of room-temperature density which decrease with increasing temperature of cure; this is presumably a consequence of the conversion at vitrification increasing at higher cure temperatures. A summary of the room temperature stress vs. cure time (Fig. 18) also shows a similar result.

The anomalous changes in the developed stress at room temperature have been discussed in terms of density changes and have neglected modulus changes. However, since anomalous changes in density parallel similar changes in modulus, the bending of the composite bi-layer specimen is affected by density and modulus in the same manner.

These anomalous changes in RT stress are to be anticipated in view of the discussion of the introduction.

CONCLUSIONS

The results of this preliminary study show that the RT stresses developed in a composite specimen, consisting of an epoxy film coated on a silicon wafer, pass through a maximum with increasing extent of cure. This anomalous behavior corresponds to parallel behavior of RT density and RT modulus, and to the increase in RT equilibrium moisture absorption, vs. extent of cure in neat epoxy systems.

The underlying reason for these phenomena is explained in terms of anomalous free volume changes. The latter arise from the incremental shrinkage at a given temperature of cure being smaller than the corresponding loss of contraction on cooling to RT at higher conversions, since T_g increases more than expected at higher extents of cure due to the non-linear relationship between T_g and conversion. Consequently, the specific volume at RT increases with increasing T_g and the RT density and stress decrease.

The anomalous behavior of room temperature stress and room temperature density versus extent of cure should be of concern in the design and use of composite materials which have, as one component, a crosslinking thermosetting polymer.

REFERENCES

1. J. K. Gillham, Polym. Eng. Sci. 26, 1429 (1986).

2. J. K. Gillham in "Developments in Polymer Characterisation", J. V. Dawkins, ed., Vol. 3, Ch. 5, pp. 159-227. Applied Science Publishers, Ltd., London (1982).

3. J. B. Enns and J. K. Gillham, J. Appl. Polym. Sci. 28, 2831 (1983).

4. M. T. Aronhime, X. Peng, and J. K. Gillham, J. Appl. Polym. Sci. 32, 3589 (1986).

5. A. Shimazaki, J. Polym. Sci., Part C 23, 555 (1968).

6. K. P. Pang and J. K. Gillham, J. Appl. Polym. Sci. 37, 1969 (1989).

7. K. P. Pang, "Anomalous Behavior of Density and Mechanical Properties of Thermosetting Polymers with Increasing Conversion". Ph.D. Thesis, Princeton University (1988).

8. M. Shimbo, M. Ochi, and J. Shigeta, J. Appl. Polym. Phys. 26, 2265 (1981).

9. E. P. EerNisse, Appl. Phys. Lett. 35, 8 (1979).

10. G. G. Stoney, Proc. Roy. Soc. A82, 172 (1909).

11. J. D. Wilcock, and D. S. Campbell, Thin Solid Films, 3, 3 (1969).

12. H. Lee and K. Neville, "Handbook of Epoxy Resins", McGraw-Hill Inc. (1967).

13. E. P. EerNisse, Appl. Phys. Lett. 30, 290 (1977).

14. M. J. Sanders, Rev. Sci. Instrum. 44, 330 (1973).

15. G. Wisanrakkit, Ph.D. Thesis, Princeton University, 1990.

16. J. K. Gillham, Applied Polymer Symposia, 2, pp. 45-58 (1966).

ACKNOWLEDGEMENTS. Financial support has been provided principally by the Office of Naval Research. One of us (MAT) acknowledges support during the summer of 1988 by AT&T Bell Laboratories in Princeton, NJ where the apparatus was constructed and used throughout the project in the laboratory of Dr. J. A. Emerson. The authors express their gratitude to Professor B. S. Royce, Applied Physics Laboratory, Princeton University, for designing the cantilever beam apparatus. Our thanks go also to Guy Wisanrakkit for constructing and testing the cantilever beam apparatus.

FIGURE CAPTIONS

Fig. 1. Schematic isothermal time-temperature-transformation (TTT) cure diagram of a thermosetting polymer, displaying three characteristic temperatures ($T_{g\infty}$, $_{gel}T_g$, T_{go}) and distinct regions of matter [liquid, sol/gel rubber, gel rubber, sol glass, sol/gel glass, fully cured (gel) glass, and char]. The full cure contour corresponds to $T_g = T_{g\infty}$ Degradation events are devitrification and char formation.

Fig. 2. T_g vs. conversion at various T_cs (6): (■) 66.7°C; (◆) 80°C; (□) 100°C; (◇) 120°C; (■) 140°C; (x) 165°C; (+) 180°C.

Fig. 3. Schematic specific volume (V) vs. temperature (T) diagram of epoxies cured to different extents ($1 < 2 < 3$) at T_c. Note the anomalous behavior of increasing specific volume at RT with increasing T_g when $T_g >> {}_{gel}T_g$ (6). $V(T_g)$ vs. T_g for $T_g >> {}_{gel}T_g$ is represented by the dashed line.

Fig. 4. Chemical formulae of the difunctional epoxy system (DER 332/TMAB).

Fig. 5. Cantilever beam apparatus used for stress measurements.

Fig. 6. Calibration curve for density gradient column. The sensitivity and temperature of the density column were maintained at 0.0005 gm/mL cm and 24.95 ± 0.05°C, respectively.

Fig. 7. Time-temperature-transformation (TTT) cure diagram for DER 332/TMAB: (⊙) gelation; (●) vitrification. $T_{g\infty}$ = 180°C. $_{gel}T_g'$ = 35°C. Data were obtained using TBA (15).

Fig. 8. Spot separation change of the two parallel beams vs. cure time for a composite specimen at 120°C.

Fig. 9. Calculated curvature change of a composite specimen during isothermal cure at 120°C.

Fig. 10. Calculated stress developed in a composite specimen during isothermal cure at 120°C.

Fig. 11. Spot separation change during temperature scan. The specimen was allowed to cure for 1 hour at each temperature. Heating rate: 5°C/min.

Fig. 12. Calculated curvature change of a composite specimen during a temperature scan. The specimen was allowed to cure for 1 hour at each temperature.

Fig. 13. Calculated stress developed during a temperature scan (50 to 250°C). The specimen was allowed to cure for 1 hour at each temperature. Heating rate: 5°C/min.

Fig. 14. RT stress change vs. cure time at 120°C for a series of specimens. Cooling rate: ca. 5°C/min.

Fig. 15. RT stress change vs. cure time at 130°C for a series of specimens. Cooling rate: ca. 5°C/min.

Fig. 16. RT stress change vs. cure time at 140°C for a series of specimens. Cooling rate: Ca. 5°C.

Fig. 17. RT stress change vs. cure time at 160°C for a series of specimens. Cooling rate: ca. 5°C/min.

Fig. 18. Summary: Effect of time of cure on RT stress for different isothermal cure temperatures (°C): (●) 120; (△) 130; (■) 140; (□) 160. Cooling rate: Ca. 5°C/min.

Fig. 19. RT density vs. cure time at 120°C for a series of specimens. Cooling rate: Ca. 5°C/min.

Fig. 20. RT density vs. cure time at 130°C for a series of specimens. Cooling rate: Ca. 5°C/min.

Fig. 21. RT density vs. cure time at 140°C for a series of specimens. Cooling rate: Ca. 5°C/min.

Fig. 22. RT density vs. cure time at 160°C for a series of specimens. Cooling rate: Ca. 5°C/min.

Fig. 23. Effect of time of cure on RT density for different isothermal cure temperatures (°C): (●) 120; (△) 130; (■) 140; (□)160. Cooling rate: Ca. 5°C/min.

Fig. 24. Location of specimens (DER 332/TMAB) vs. time in the density gradient column prepared from toluene and carbon tetrachloride. Specimens were cured at 120°C for different times (hr): (○) 0.5; (▲) 1.0; (■) 3.0; (□) 12; (●) 168.

THE THERMOSETTING PROCESS: TIME-TEMPERATURE-TRANSFORMATION CURE DIAGRAM

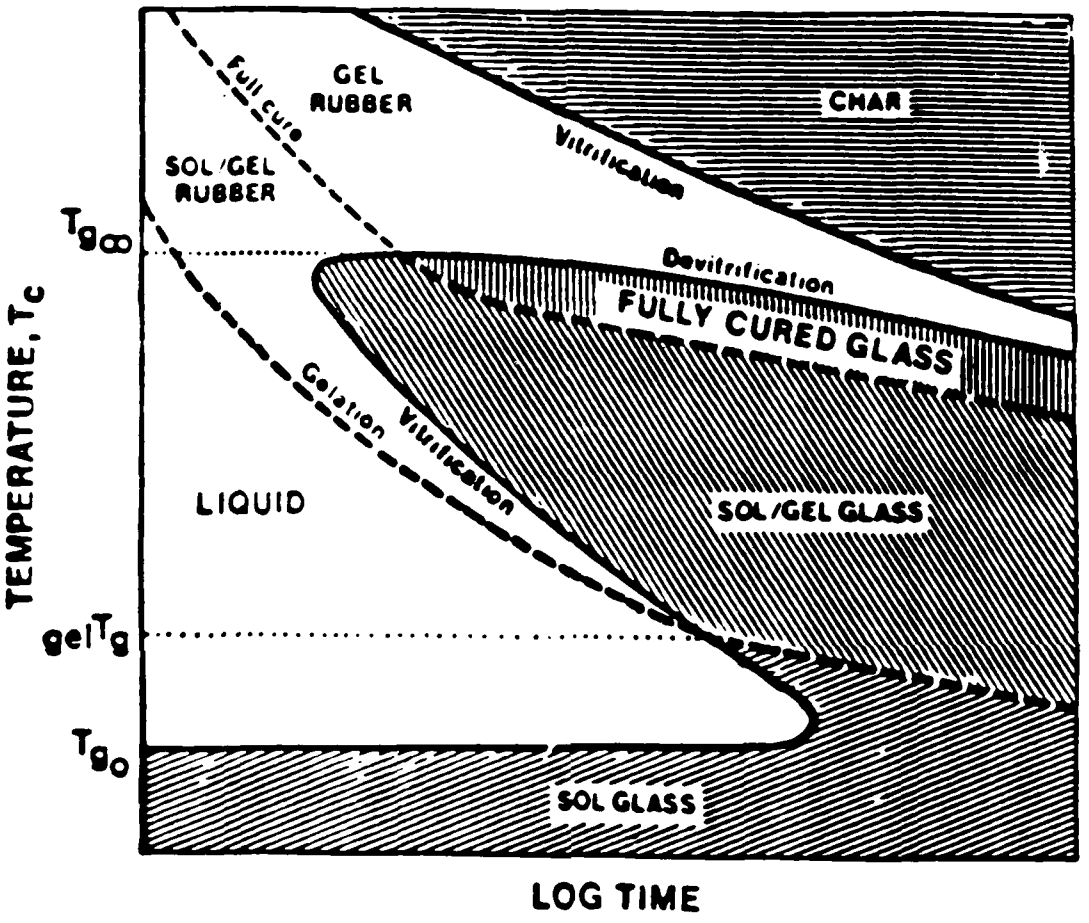

Figure 1

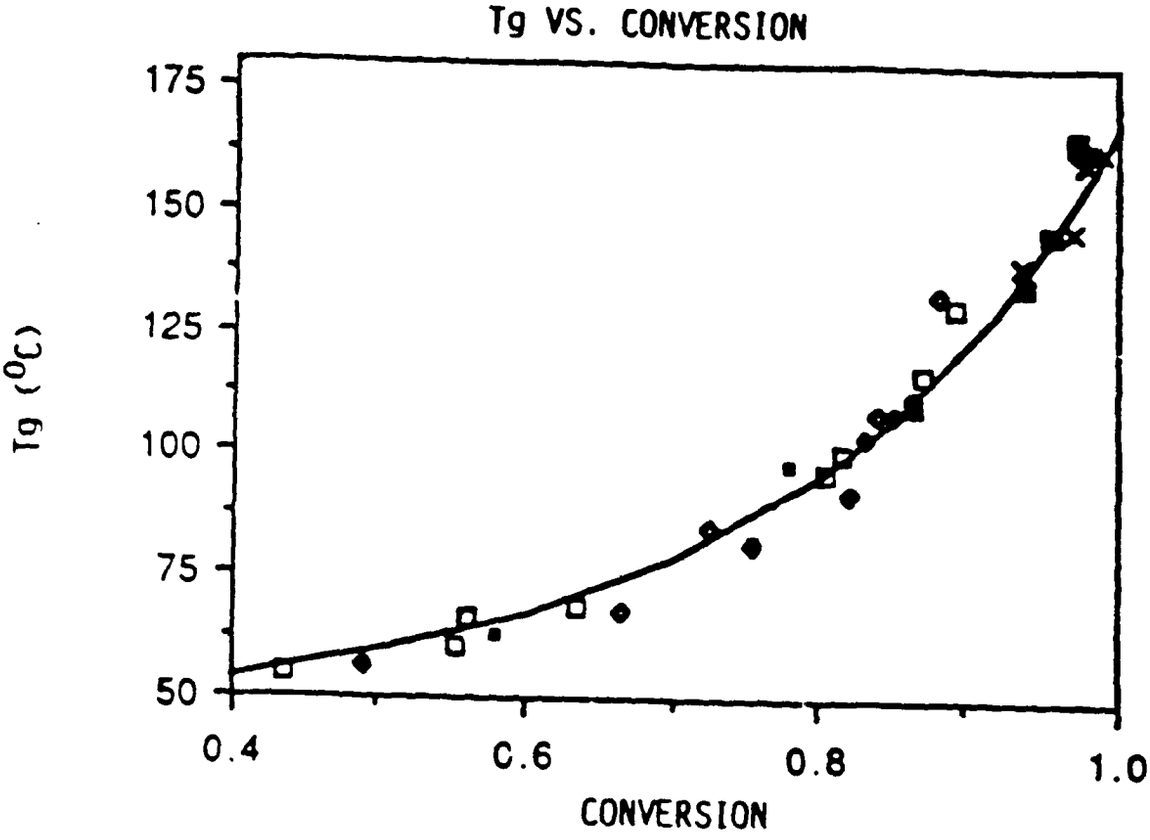
Tg VS. CONVERSION
175
150
125
100
75
50
Tg (°C)
0.4
0.6
0.8
1.0
CONVERSION

Figure 2

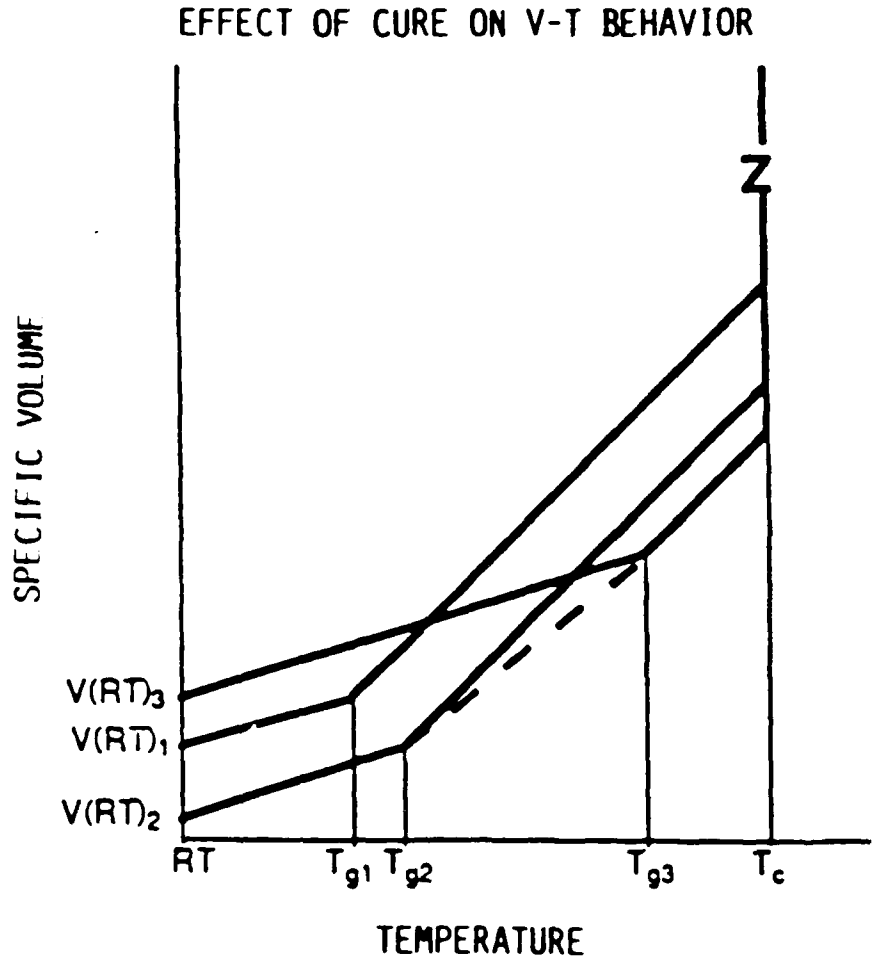
EFFECT OF CURE ON V-T BEHAVIOR
Z
SPECIFIC VOLUME
V(RT)3
V(RT)1
V(RT)2
RT
Tg1
Tg2
Tg3
Tc
TEMPERATURE

Figure 3

CHEMICAL FORMULAE

Diglycidyl Ether of Bisphenol A (DER 332)

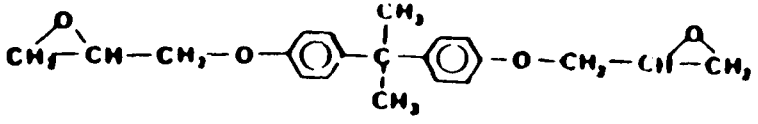

Trimethylene Glycol Di-p-aminobenzoate (TMAD)

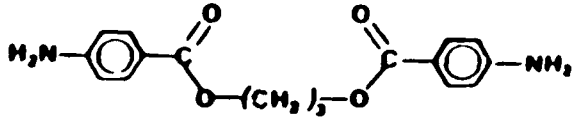

Figure 4

CANTILEVER BEAM APPARATUS

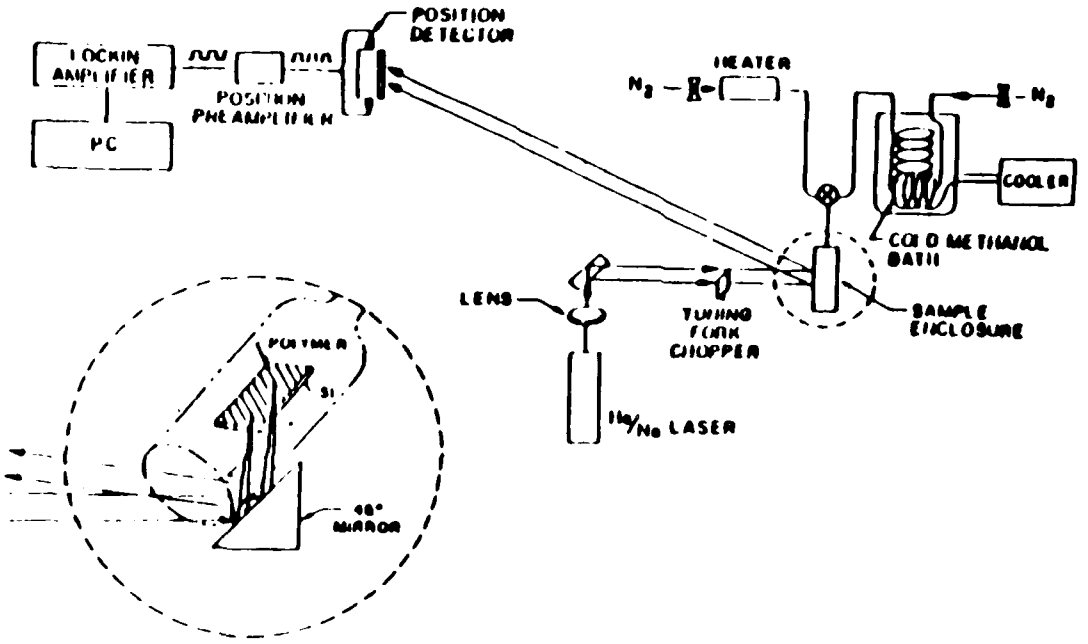

Figure 5

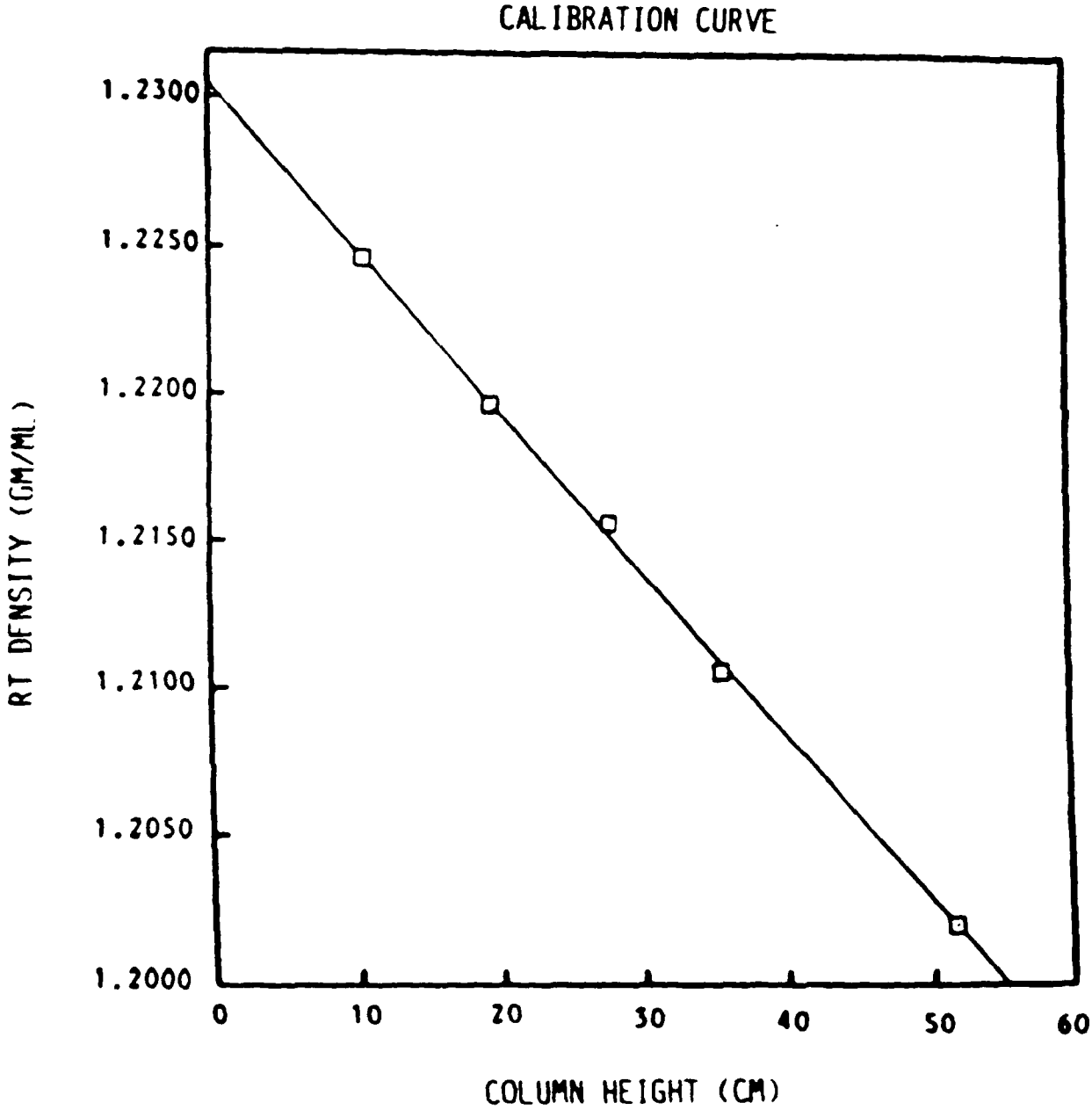
CALIBRATION CURVE
RT DENSITY (GM/ML)
1.2300
1.2250
1.2200
1.2150
1.2100
1.2050
1.2000
0
10
20
30
40
50
60
COLUMN HEIGHT (CM)

Figure 6

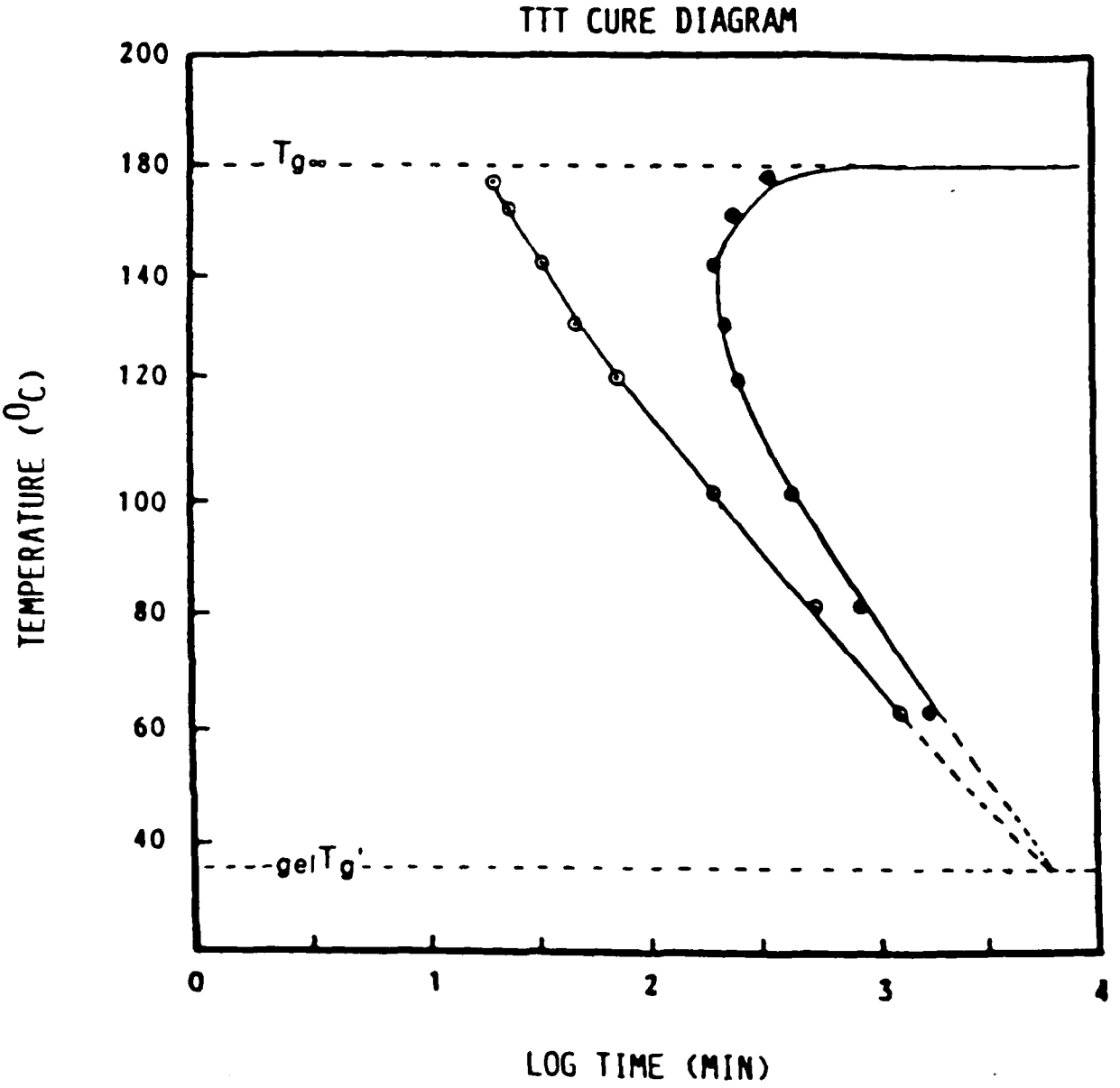
TTT CURE DIAGRAM
200
180
140
120
100
80
60
40
$T_{g\infty}$
gel T_g
TEMPERATURE (^{0}C)
0
1
2
3
4
LOG TIME (MIN)

Figure 7

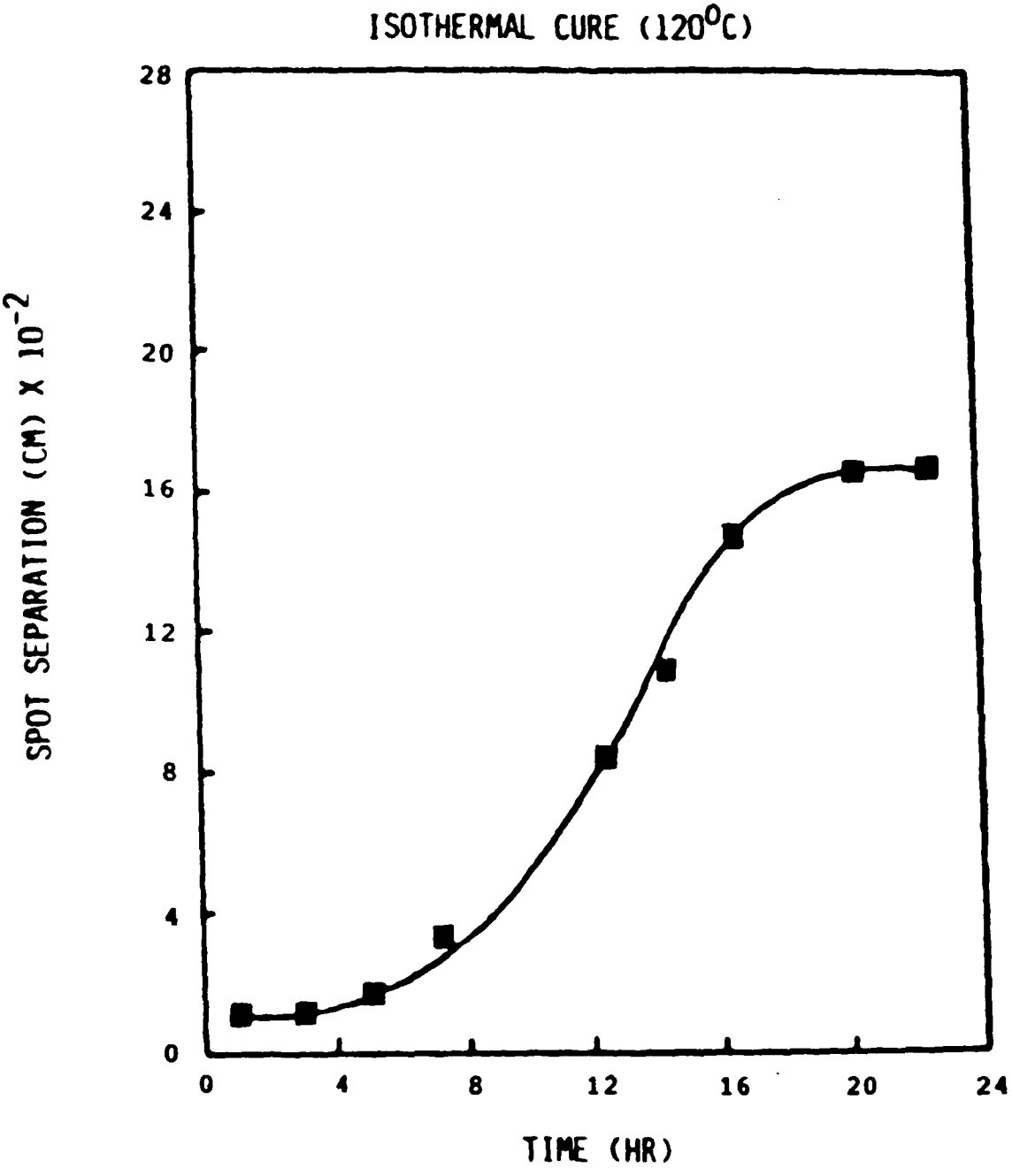
ISOTHERMAL CURE (120°C)
SPOT SEPARATION (CM) X 10^{-2}
28
24
20
16
12
8
4
0
0
4
8
12
16
20
24
TIME (HR)

Figure 8

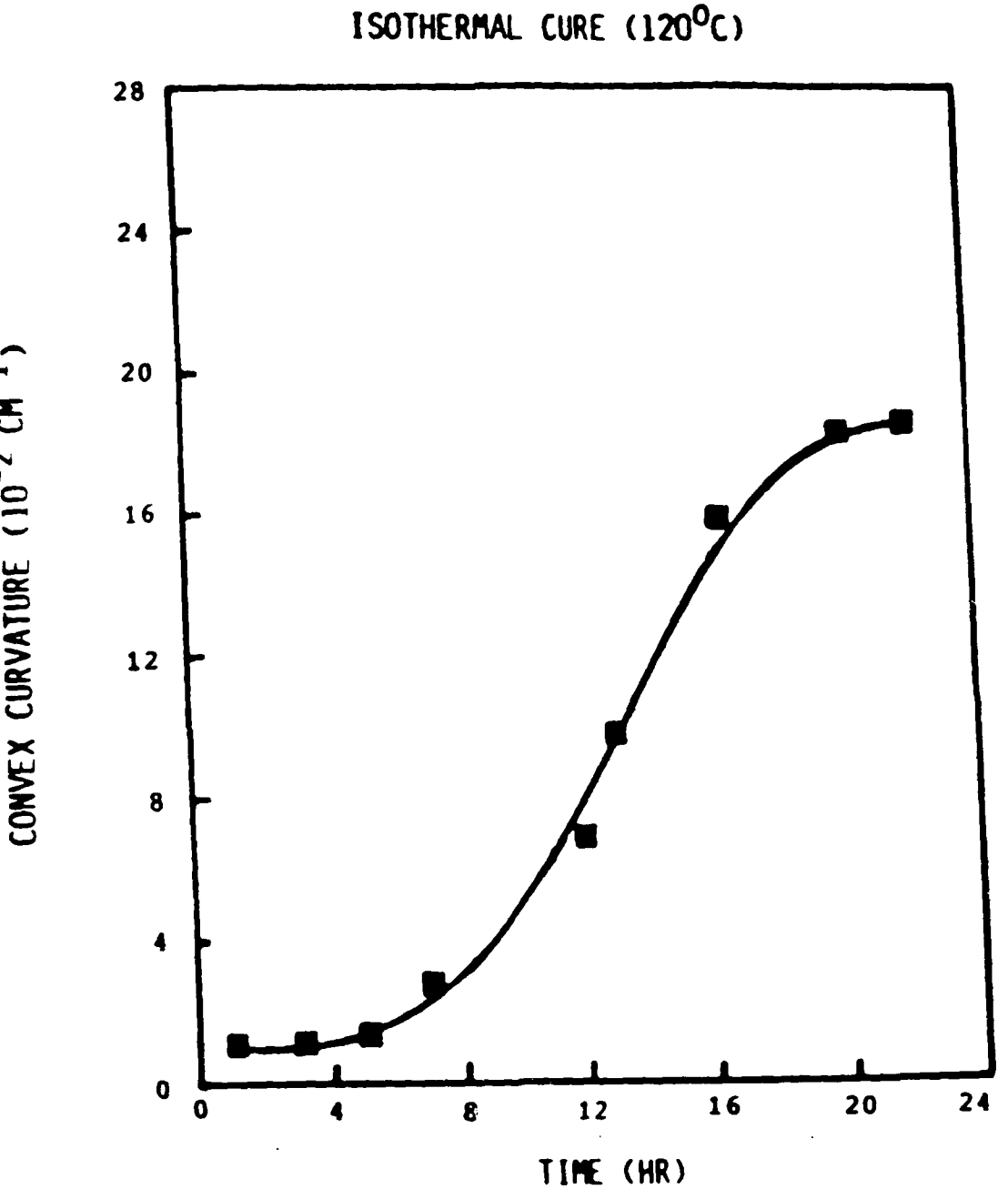
ISOTHERMAL CURE (120°C)
CONVEX CURVATURE (10^{-2} CM^{-1})
28
24
20
16
12
8
4
0
0
4
8
12
16
20
24
TIME (HR)

Figure 9

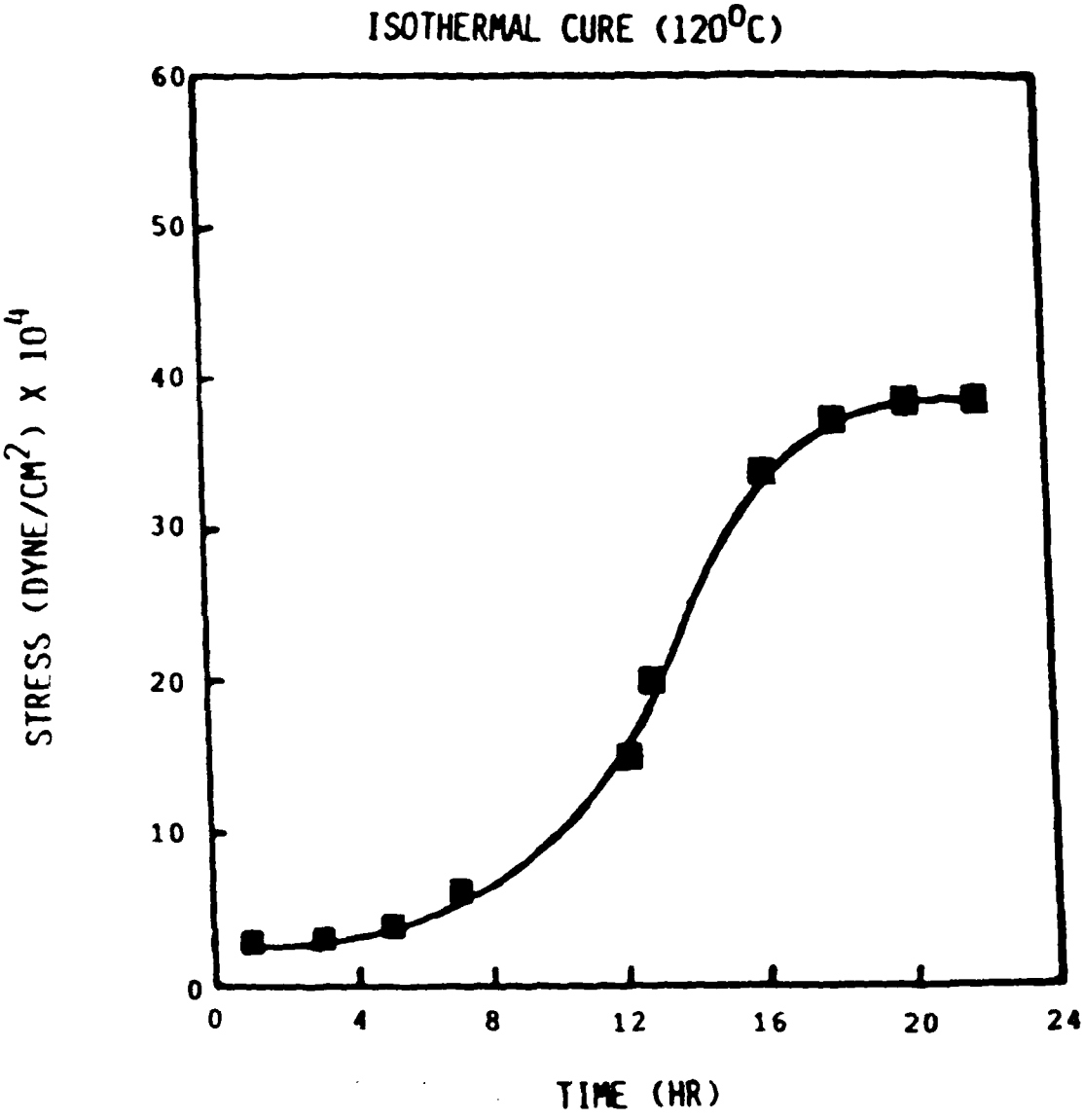
ISOTHERMAL CURE (120°C)
STRESS (DYNE/CM²) X 10⁴
60
50
40
30
20
10
0
0
4
8
12
16
20
24
TIME (HR)

Figure 10

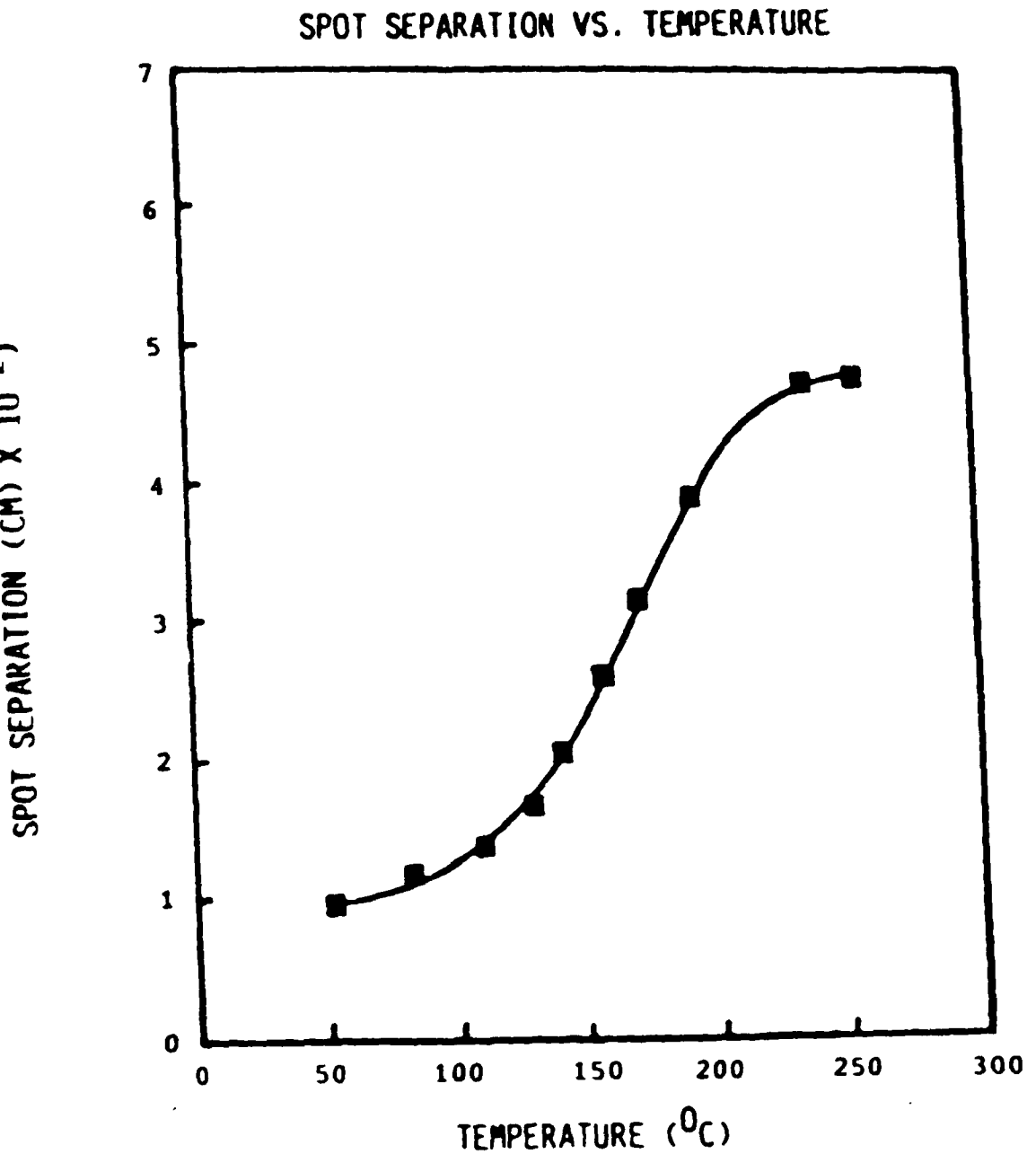
SPOT SEPARATION VS. TEMPERATURE
SPOT SEPARATION (CM) X 10^{-2}
TEMPERATURE (^{0}C)
0
1
2
3
4
5
6
7
0
50
100
150
200
250
300

Figure 11

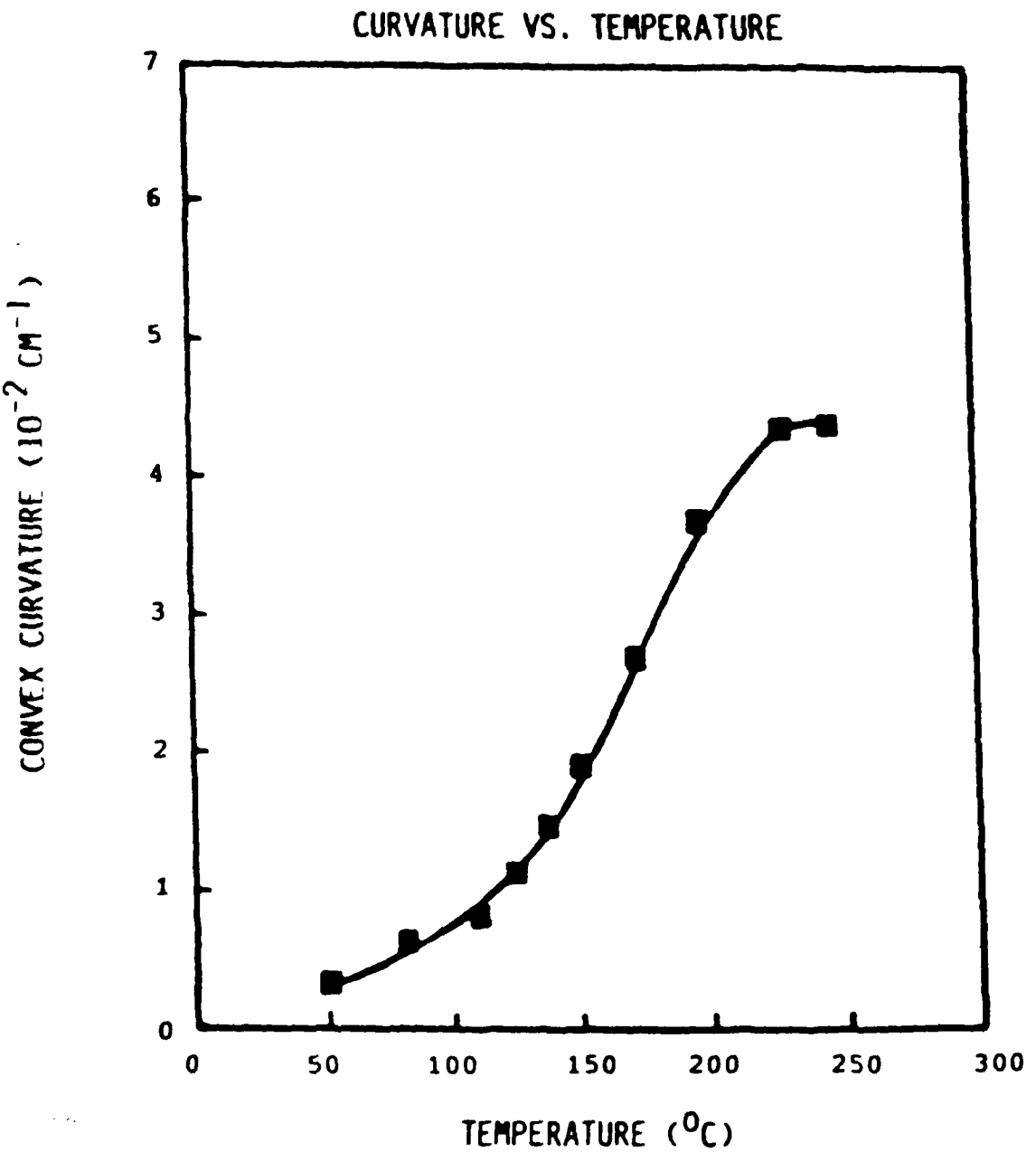
CURVATURE VS. TEMPERATURE
CONVEX CURVATURE (10^{-2} CM^{-1})
0
1
2
3
4
5
6
7
0
50
100
150
200
250
300
TEMPERATURE (^{O}C)

Figure 12

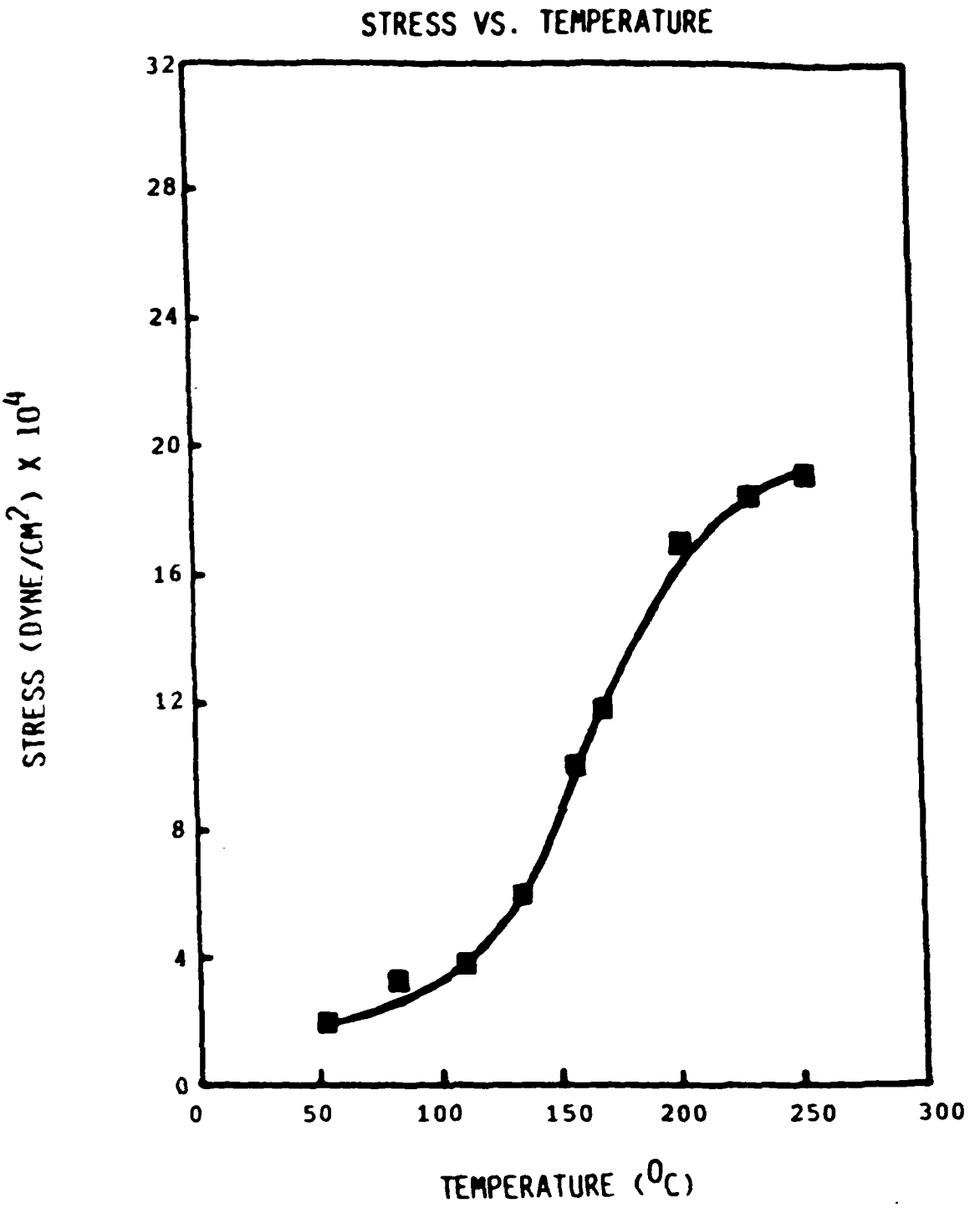
STRESS VS. TEMPERATURE
STRESS (DYNE/CM^2) X 10^4
32
28
24
20
16
12
8
4
0
0
50
100
150
200
250
300
TEMPERATURE (^{0}C)

Figure 13

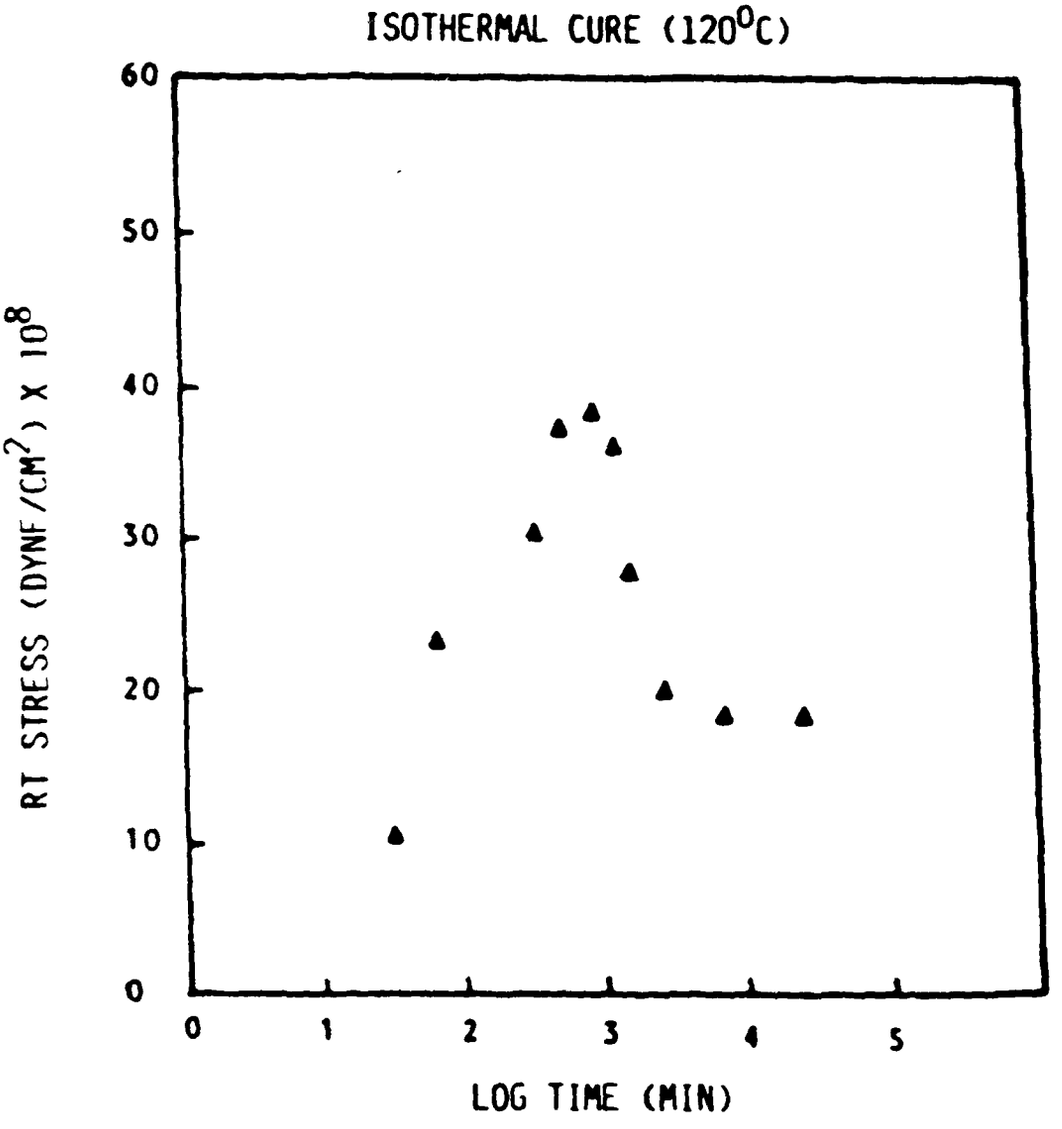
ISOTHERMAL CURE (120°C)
RT STRESS (DYNF/CM²) X 10⁸
60
50
40
30
20
10
0
0
1
2
3
4
5
LOG TIME (MIN)

Figure 14

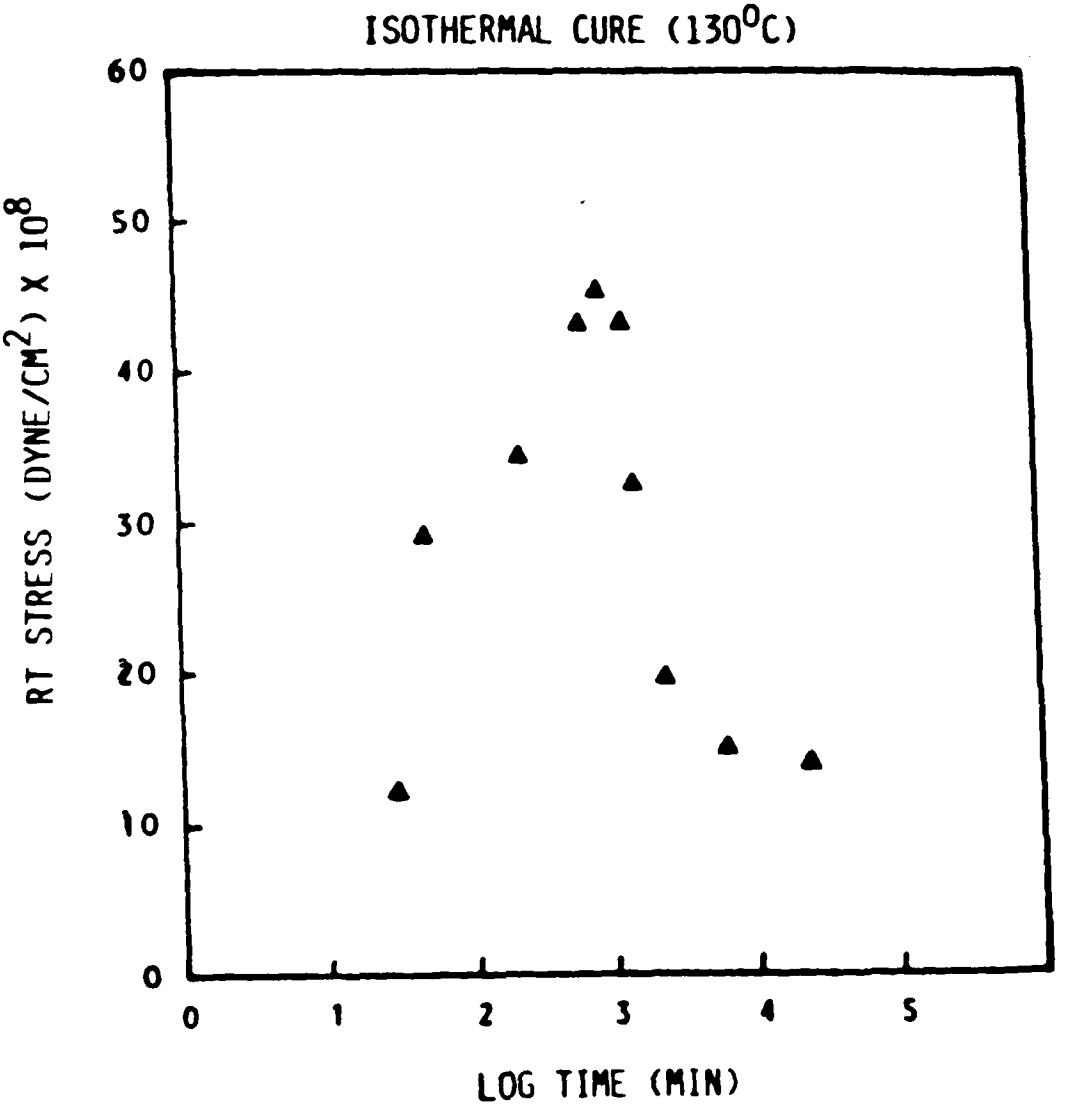
ISOTHERMAL CURE (130°C)
RT STRESS (DYNE/CM²) X 10⁸
60
50
40
30
20
10
0
0
1
2
3
4
5
LOG TIME (MIN)

Figure 15

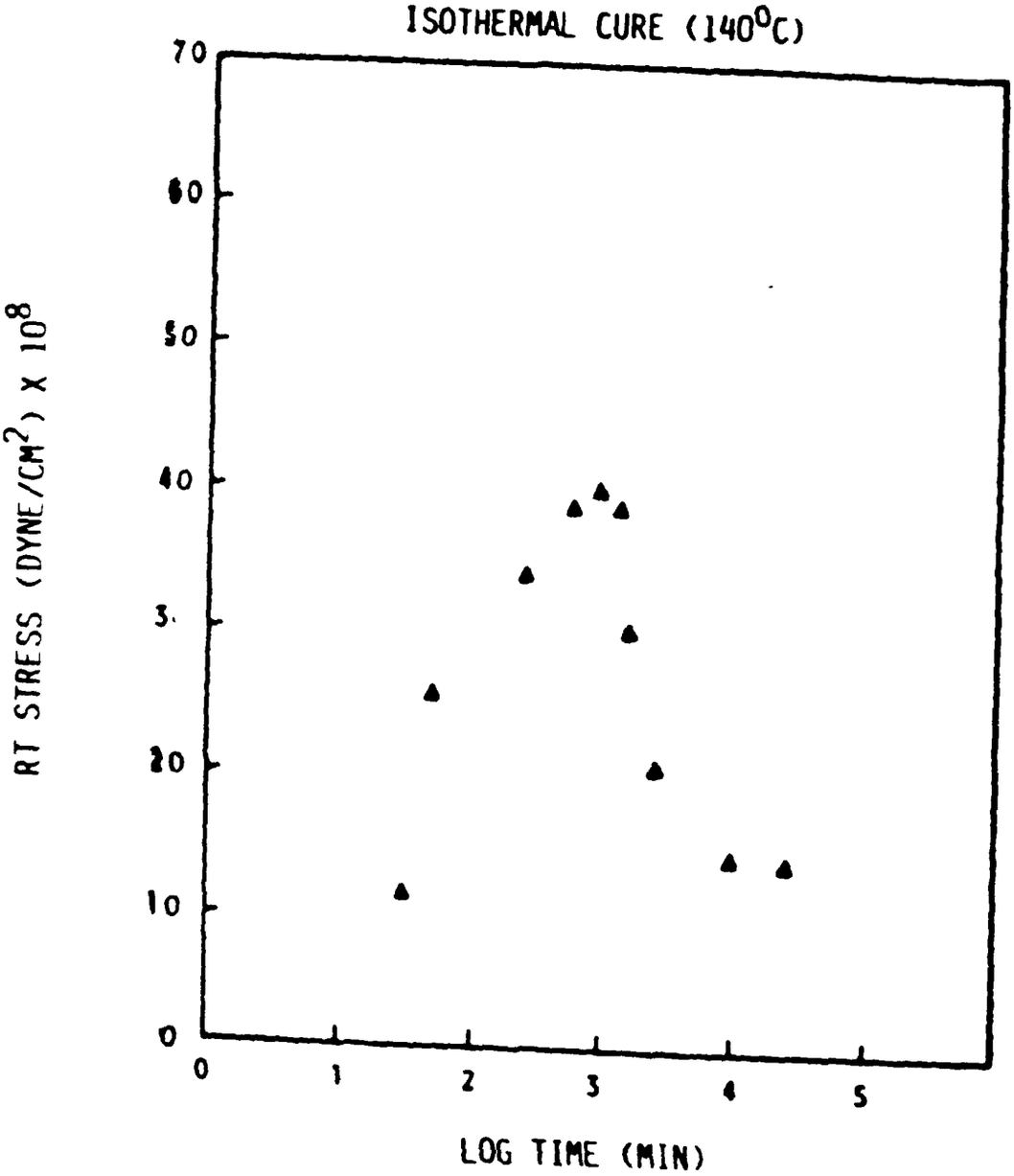
ISOTHERMAL CURE (140°C)
RT STRESS (DYNE/CM²) X 10⁸
70
60
50
40
30
20
10
0
0
1
2
3
4
5
LOG TIME (MIN)

Figure 16

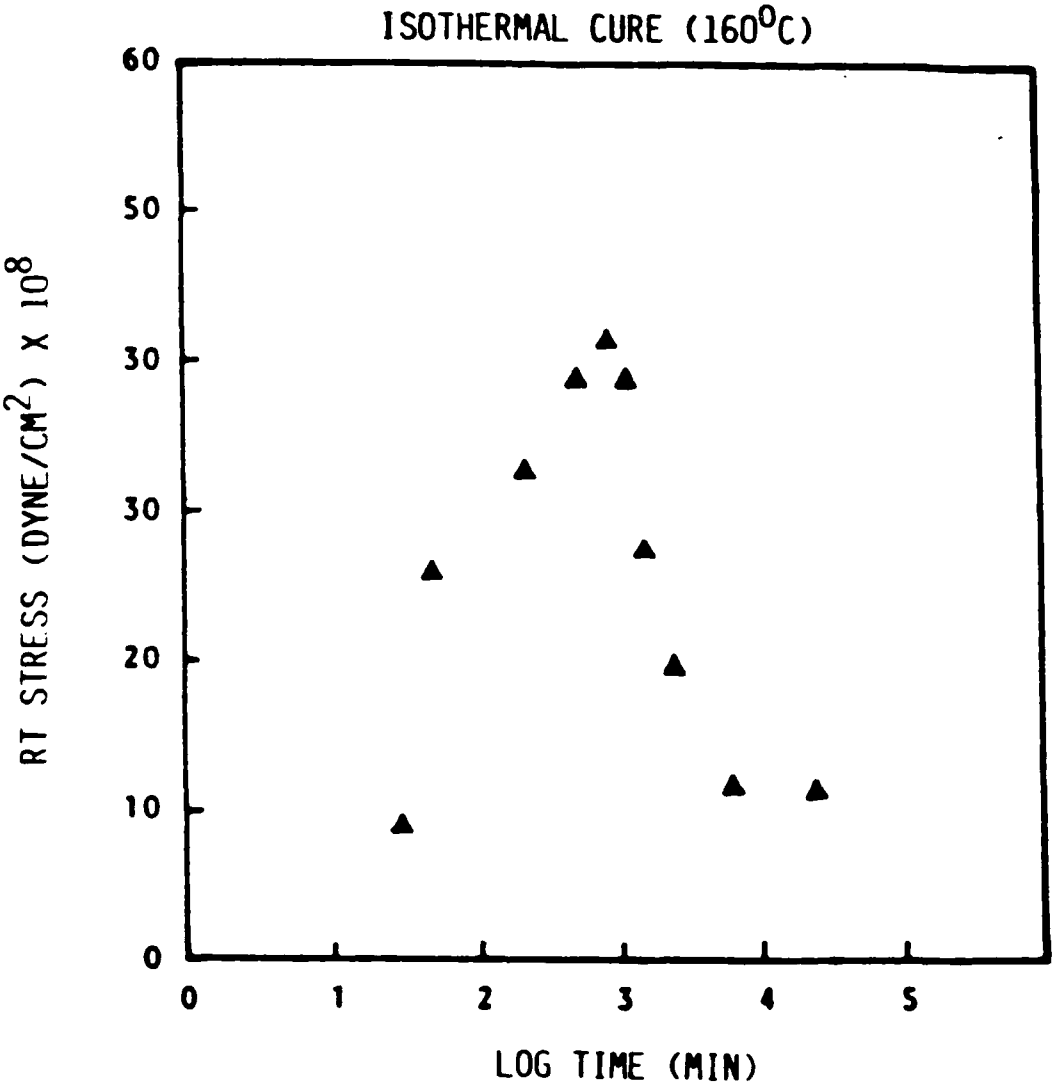
ISOTHERMAL CURE (160°C)
RT STRESS (DYNE/CM²) X 10⁸
60
50
30
30
20
10
0
0
1
2
3
4
5
LOG TIME (MIN)

Figure 17

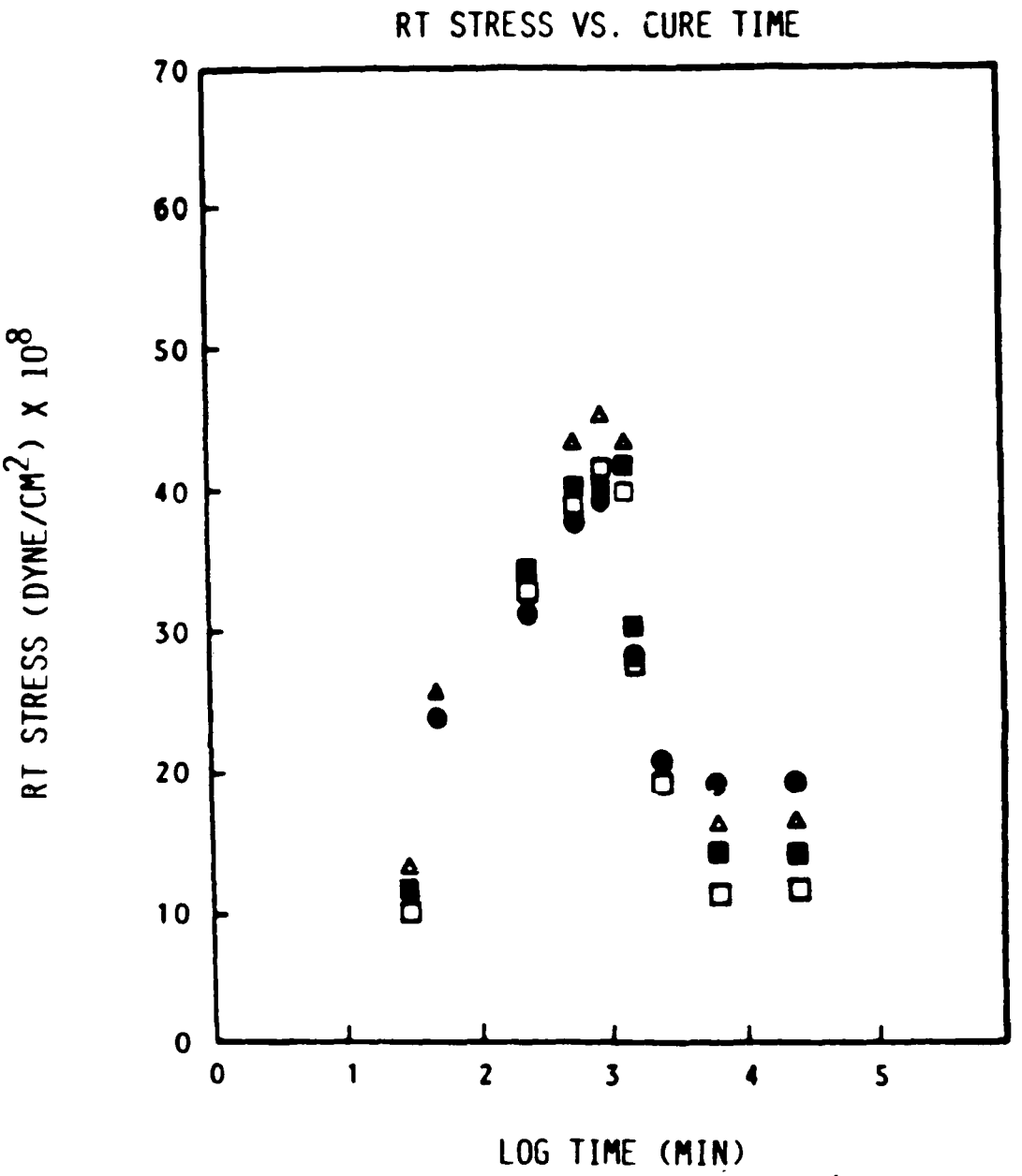
RT STRESS VS. CURE TIME
RT STRESS (DYNE/CM^2) X 10^8
70
60
50
40
30
20
10
0
0
1
2
3
4
5
LOG TIME (MIN)

Figure 18

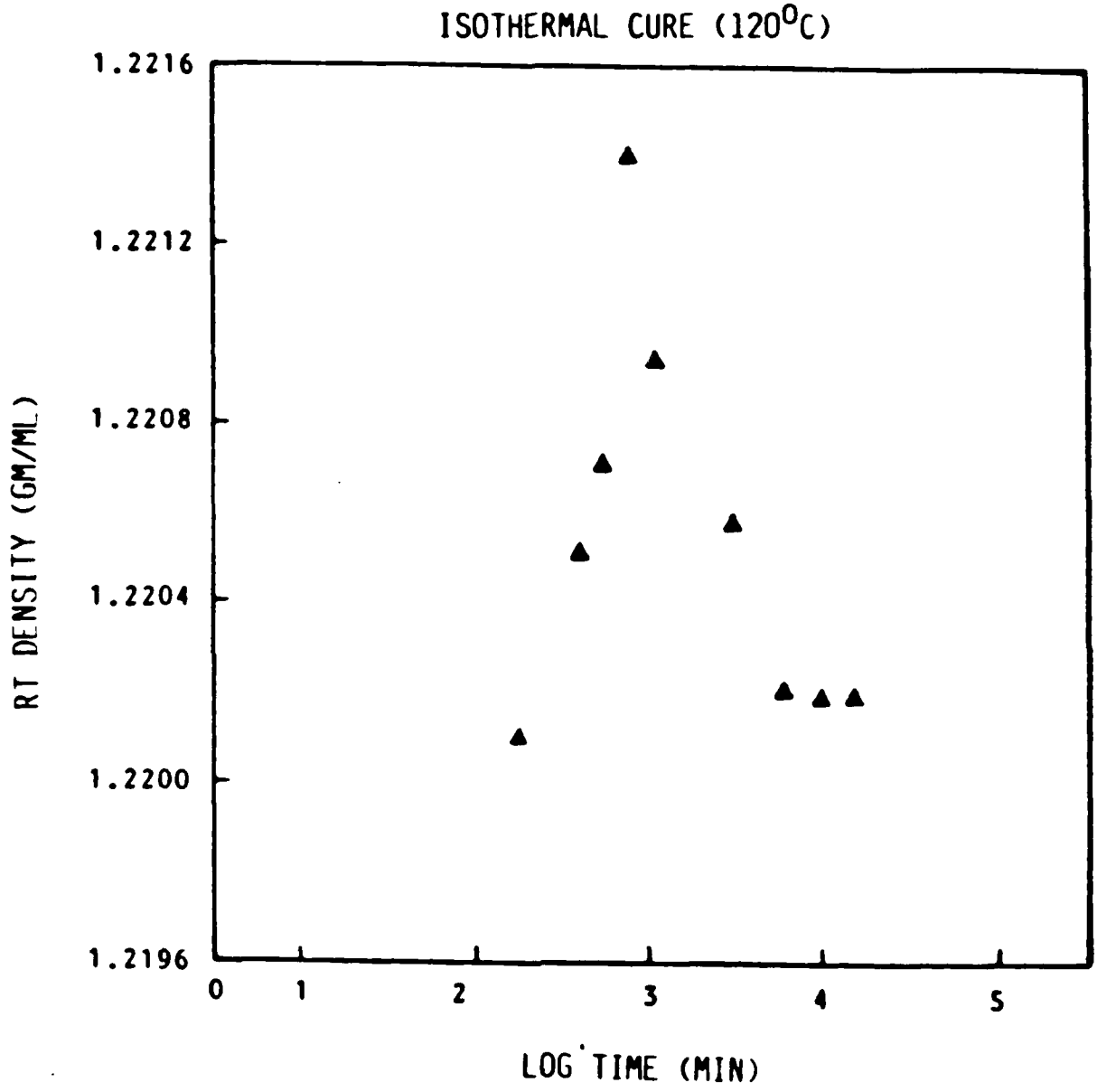
ISOTHERMAL CURE (120°C)
1.2216
1.2212
1.2208
1.2204
1.2200
1.2196
RT DENSITY (GM/ML)
0
1
2
3
4
5
LOG TIME (MIN)

Figure 19

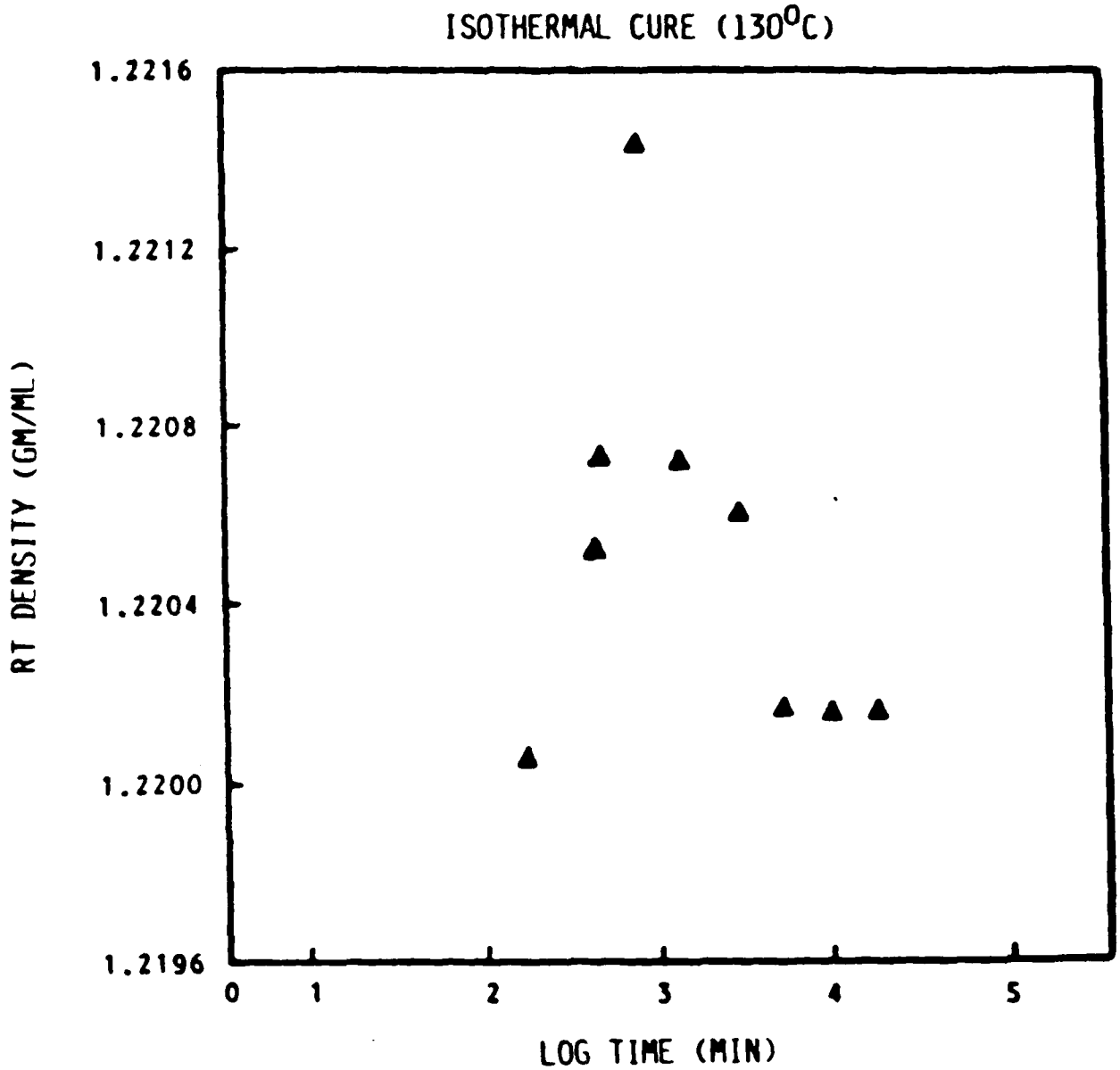
ISOTHERMAL CURE (130°C)
1.2216
1.2212
1.2208
1.2204
1.2200
1.2196
RT DENSITY (GM/ML)
0
1
2
3
4
5
LOG TIME (MIN)

Figure 20

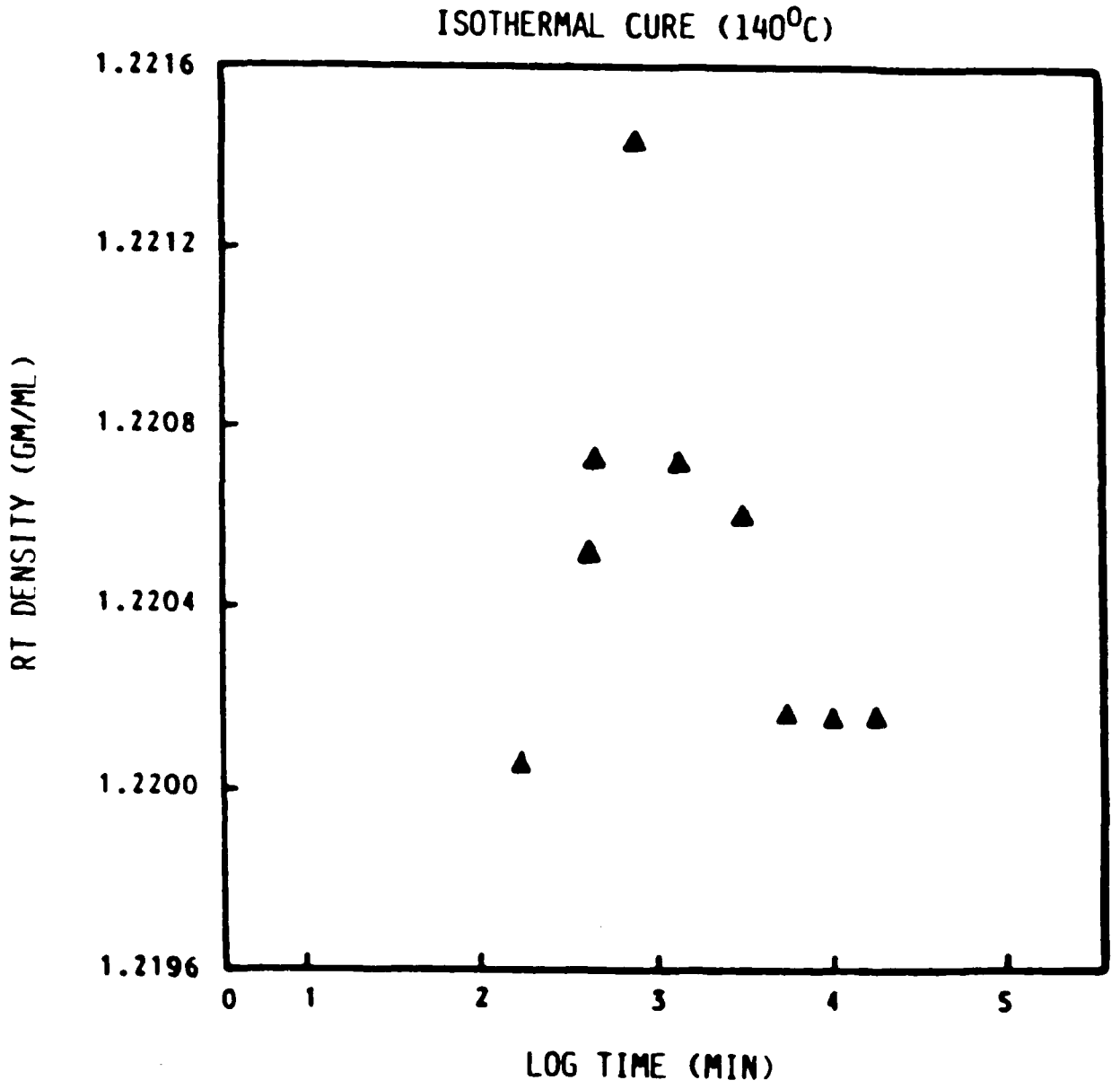
ISOTHERMAL CURE (140°C)
1.2216
1.2212
1.2208
1.2204
1.2200
1.2196
RT DENSITY (GM/ML)
0
1
2
3
4
5
LOG TIME (MIN)

Figure 21

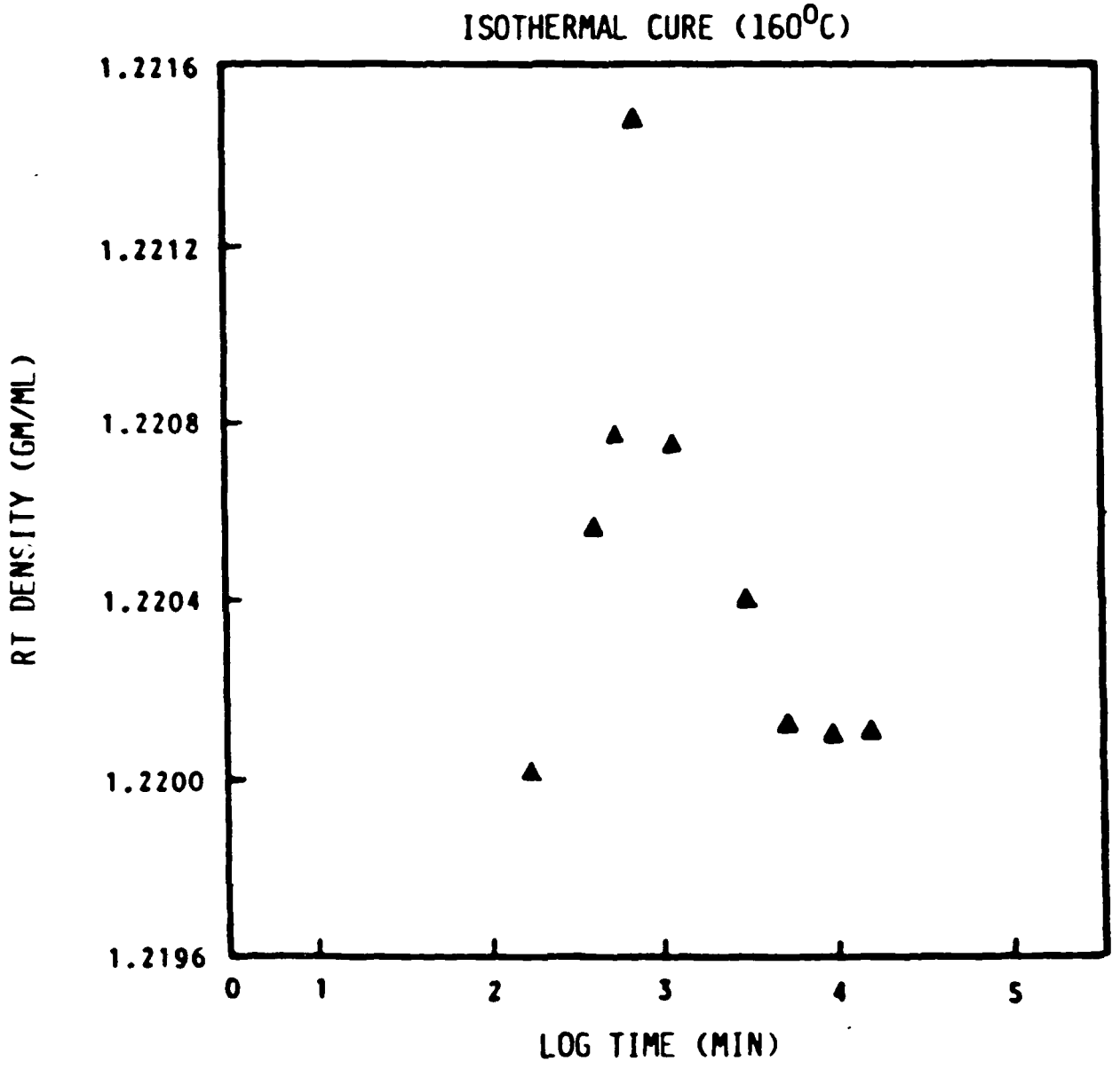
ISOTHERMAL CURE (160°C)
1.2216
1.2212
1.2208
1.2204
1.2200
1.2196
RT DENSITY (GM/ML)
0
1
2
3
4
5
LOG TIME (MIN)

Figure 22

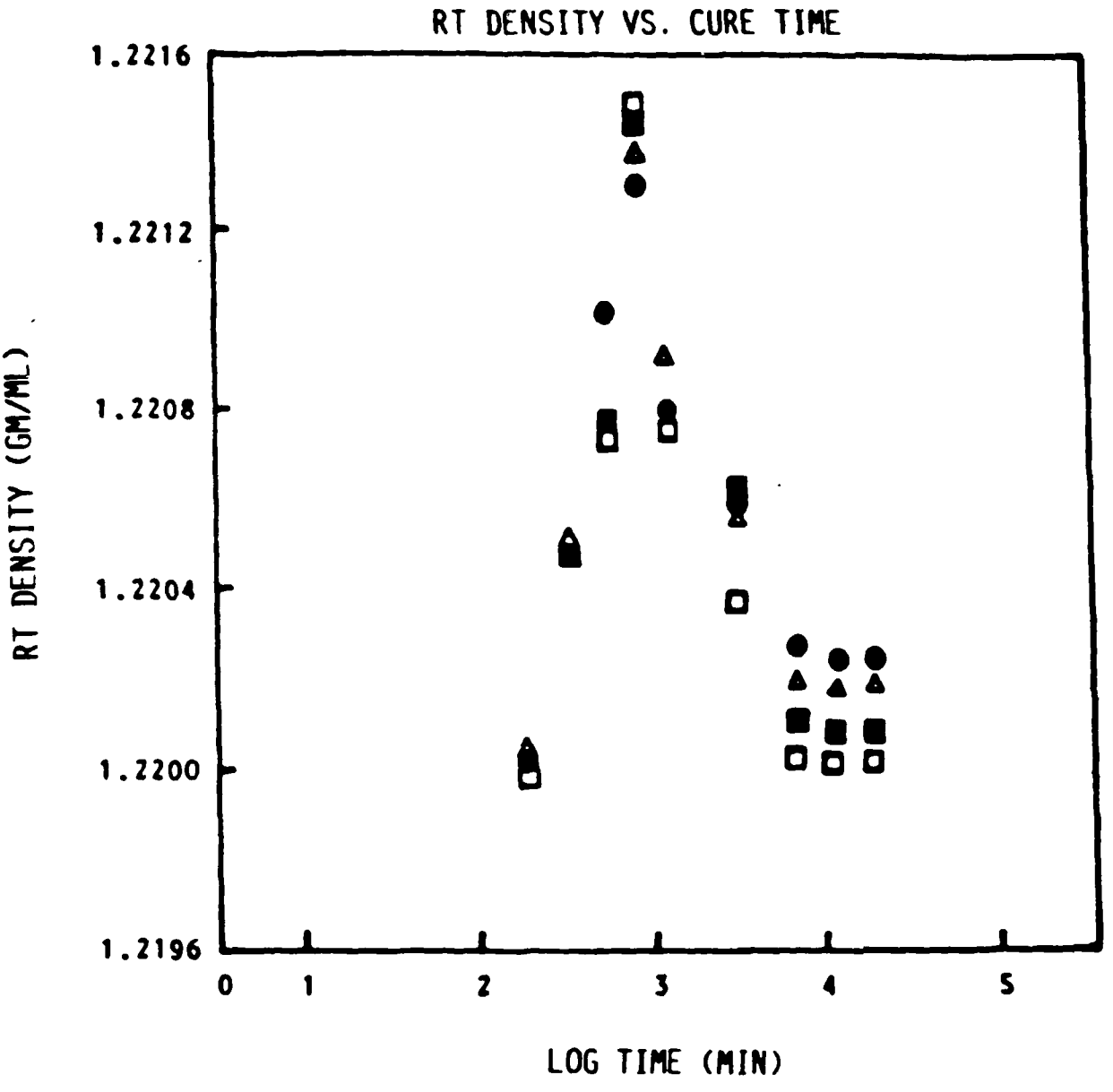
RT DENSITY VS. CURE TIME
1.2216
1.2212
1.2208
1.2204
1.2200
1.2196
RT DENSITY (GM/ML)
0
1
2
3
4
5
LOG TIME (MIN)

Figure 23

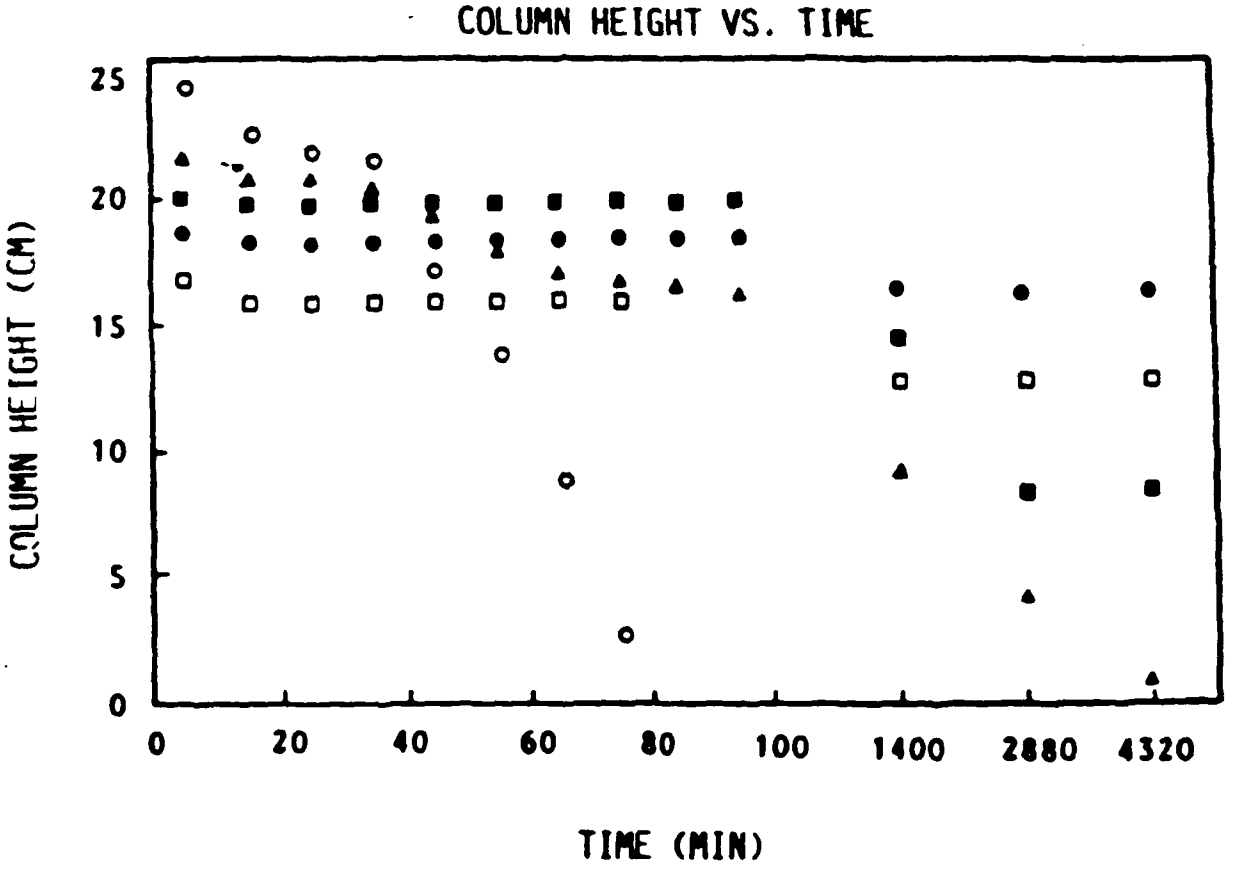
COLUMN HEIGHT VS. TIME
COLUMN HEIGHT (CM)
25
20
15
10
5
0
0
20
40
60
80
100
1400
2880
4320
TIME (MIN)

Figure 24

DL/1113/87/2

TECHNICAL REPORT DISTRIBUTION LIST, GEN

	No. Copies
Office of Naval Research Attn: Code 1113 800 N. Quincy Street Arlington, Virginia 22217-5000	2
Dr. Bernard Douda Naval Weapons Support Center Code 50C Crane, Indiana 47522-5050	1
Naval Civil Engineering Laboratory Attn: Dr. R. W. Drisko, Code L52 Port Hueneme, California 93401	1
Defense Technical Information Center Building 5, Cameron Station Alexandria, Virginia 22314	12 high quality
DTNSRDC Attn: Dr. H. Singerman Applied Chemistry Division Annapolis, Maryland 21401	1
Dr. William Tolles Superintendent Chemistry Division, Code 6100 Naval Research Laboratory Washington, D.C. 20375-5000	1
Dr. David Young Code 334 NORDA NSTL, Mississippi 39529	1
Naval Weapons Center Attn: Dr. Ron Atkins Chemistry Division China Lake, California 93555	1
Scientific Advisor Commandant of the Marine Corps Code RD-1 Washington, D.C. 20380	1
U.S. Army Research Office Attn: CRD-AA-IP P.O. Box 12211 Research Triangle Park, NC 27709	1
Mr. John Boyle Materials Branch Naval Ship Engineering Center Philadelphia, Pennsylvania 19112	1
Naval Ocean Systems Center Attn: Dr. S. Yamamoto Marine Sciences Division San Diego, California 91232	1